

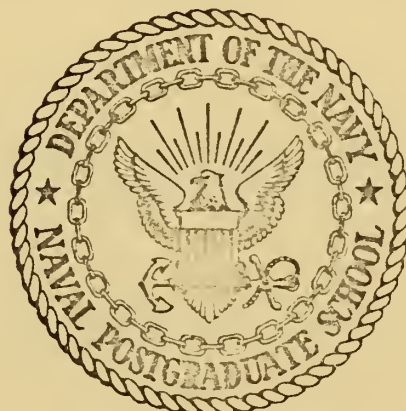
BUBBLE DISTRIBUTIONS IN A QUIESCENT OCEAN  
CALCULATED FROM THE BUBBLE TRANSPORT EQUATION

Thomas Carl Vajda



# NAVAL POSTGRADUATE SCHOOL

## Monterey, California



# THESIS

BUBBLE DISTRIBUTIONS IN A QUIESCENT OCEAN  
CALCULATED FROM THE BUBBLE TRANSPORT EQUATION

by

Thomas Carl Vajda

Thesis Advisor:

G. A. Garrettson

June 1972

TL 47-94

Approved for public release; distribution unlimited.



Bubble Distributions in a Quiescent Ocean  
Calculated from the Bubble Transport Equation

by

Thomas Carl Vajda  
Lieutenant, United States Navy  
B.S., University of California at Los Angeles, 1965

Submitted in partial fulfillment of the  
requirements for the degree of

MASTER OF SCIENCE IN PHYSICS

from the  
NAVAL POSTGRADUATE SCHOOL  
June 1972

✓ 25°  
C.

## ABSTRACT

A bubble transport equation was developed and a formal solution obtained for the bubble distribution function. The distribution function obtained depends upon the model used for bubble drag, gas diffusion, and ocean circulation. As a specific application, solutions were obtained for a one-dimensional, quiescent, steady state ocean with a bottom source at 197 meters. The characteristic equations were integrated numerically to test the accuracy of approximate analytical solutions. The calculated bubble densities were compared with experimental data available for this problem. When gas diffusion is neglected, the theoretical and experimental distributions are in general agreement.



## TABLE OF CONTENTS

I.	INTRODUCTION	4
II.	THE BUBBLE TRANSPORT EQUATION	5
III.	FORMAL SOLUTION TO THE BUBBLE TRANSPORT EQUATION	8
IV.	THE MODEL FOR THE SOLUTION OF THE BUBBLE TRANSPORT EQUATION	9
	A. THE BUBBLE RADIUS CHANGE RATE	9
	B. THE BUBBLE EQUATION OF MOTION AND ACCELERATION	11
	C. BUBBLE SOURCES	13
V.	RESULTS	15
VI.	CONCLUSIONS	24
	COMPUTER OUTPUT	38
	COMPUTER PROGRAM	46
	LIST OF REFERENCES	50
	INITIAL DISTRIBUTION LIST	51
	FORM DD 1473	52



## I. INTRODUCTION

Studies have been made by many researchers regarding the mechanisms of gas bubble dynamics in a fluid from both the theoretical [Ref. 1] and the experimental [Refs. 2, 3, and 4] aspects. The mechanisms of gas bubble formation, transport, and extinction are important as gas bubbles can effect the propagation of sound in the ocean by the under-water scattering of sound beams. Theoretical studies have explained how a bubble varies in size as it rises in a quiescent fluid. The phenomena involved includes shrinkage from gas diffusion versus expansion from decreasing hydrostatic pressure and shrinkage from surface tension for very small bubbles. However, there does not appear to be at present any theory explaining how the distribution of bubbles generated by a bottom or distributed source in the ocean can be expected to vary with depth or initial bubble radius.

This paper outlines the theory for determining theoretically the distributions of bubbles generated by a bottom source in the ocean [Ref. 5]. First, a linear bubble transport equation is developed and then it is solved by the method of characteristics. A model for a one-dimensional steady state ocean is specified for application of this theory. Depending on the assumptions made regarding the dynamics involved in the bubble motion, such as the importance of gas diffusion or surface tension, various semi-analytical solutions can be obtained for the distribution of bubbles from a bottom source. These distributions are then compared to available experimental data. In particular, the distributions from a bottom source located at 197 meters were calculated using various approximations and the results were compared with the experimental data in Ref. 4.



## II. THE BUBBLE TRANSPORT EQUATION

The transport equation is basically a balance equation [Refs. 6 and 7]. It was desired to develop a transport equation for the description of the distribution of bubbles as a function of position, velocity, size (bubble radius) and time in a circulating field that may contain sources or sinks. A distribution function that describes the bubble population can be defined and if the bubbles satisfy the following general assumptions, this distribution will satisfy a Boltzmann-type transport equation:

- (1) The bubbles are completely independent of one another;
- (2) If bubble interaction occurs, no more than two bubbles will interact at any one time.

Since bubbles in the ocean exact no force on one another and the history of one bubble does not affect the history of another bubble, the two above assumptions hold and a transport equation was found.

If  $\psi(\vec{r}, \vec{v}, \ell, t) d^3 r d^3 v d\ell$  is the number of bubbles at time  $t$  with radius  $d\ell$  about  $\ell$ , velocity  $d^3 v$  about  $\vec{v}$ , and position  $d^3 r$  about  $\vec{r}$ , then at time  $t' \equiv t + dt$ ,  $\psi(\vec{r}', \vec{v}', \ell', t') d^3 r' d^3 v' d\ell'$  is the number of bubbles at time  $t + dt$  with radius  $d\ell'$  about  $\ell'$ , velocity  $d^3 v'$  about  $\vec{v}'$ , and position  $d^3 r'$  about  $\vec{r}'$ , where  $\vec{r}'$ ,  $\vec{v}'$ , and  $\ell'$  are:

$$\begin{aligned}\vec{r}' &= \vec{r} + \vec{v} dt \\ \vec{v}' &= \vec{v} + \vec{a} dt \\ \ell' &= \ell + v dt\end{aligned}\tag{1}$$

The above Taylor series expansions about time  $t$  neglects all terms of order two and higher. The changes in position, velocity, and radius



are the result of nonzero velocity  $\vec{v} \equiv \vec{dr}/dt$ , acceleration  $\vec{a} \equiv \vec{dv}/dt$ , and radius change rate  $v \equiv d\ell/dt$ , respectively..

Since the transport equation is a balance equation the number of bubbles in a volume element  $d^7\tau' \equiv d^3r'd^3v'd\ell'$  at time  $t + dt$ , must equal the number of bubbles that were in the volume  $d^7\tau \equiv d^3rd^3vd\ell$  at time  $t$  plus or minus the bubbles that were generated or removed by any internal sources or sinks. Thus an equation for the conservation of bubbles is written as:

$$\psi(\vec{r}', \vec{v}', \ell', t+dt)d^7\tau' - \psi(\vec{r}, \vec{v}, \ell, t)d^7\tau = S(\vec{r}, \vec{v}, \ell, t)d^7\tau \quad (2)$$

where  $S(\vec{r}, \vec{v}, \ell, t)d^7\tau$  is the rate at which bubbles were introduced into the volume element  $d^7\tau$  about  $(\vec{r}, \vec{v}, \ell)$  by distributed sources..

Expanding  $\psi' \equiv \psi(\vec{r}', \vec{v}', \ell', t+dt)$  in a Taylor series about  $\psi \equiv \psi(\vec{r}, \vec{v}, \ell, t)$  and keeping only terms through the first order yields:

$$\psi' = \psi + (\partial\psi/\partial t)dt + (\vec{v} + \vec{\nabla}_r\psi)dt + (\vec{a} \cdot \vec{\nabla}_v\psi)dt + v(d\psi/\partial t)dt \quad (3)$$

where

$$\vec{\nabla}_r(\cdot) \equiv \partial(\cdot)/\partial x, \partial(\cdot)/\partial y, \partial(\cdot)/\partial z$$

$$\vec{\nabla}_v(\cdot) \equiv \partial(\cdot)/\partial v_x, \partial(\cdot)/\partial v_y, \partial(\cdot)/\partial v_z$$

The volume element  $d^7\tau'$  was transformed into terms of  $d^7\tau$  by using a Jacobian. The results of this transformation yielded.

$$d^7\tau' = \frac{\partial(\vec{r}', \vec{v}', \ell')}{\partial(\vec{r}, \vec{v}, \ell)} d^7\tau \quad (4)$$

with

$$\frac{\partial(\vec{r}', \vec{v}', \ell')}{\partial(\vec{r}, \vec{v}, \ell)} = 1 + (\vec{\nabla}_v \cdot \vec{a})dt + (\partial v/\partial \ell)dt \quad (5)$$



Substituting (3), (4), and (5) into (2), dividing by  $d^7\tau dt$ .

and taking the limit  $dt \rightarrow 0$  yields the bubble transport equation

[Ref. 5]:

$$\frac{\partial \psi}{dt} + \vec{v} \cdot \vec{\nabla}_r \psi + \vec{a} \cdot \vec{\nabla}_v \psi + v \frac{\partial \psi}{dt} = - (\vec{\nabla}_v \cdot \vec{a} + \frac{\partial v}{\partial t}) \psi + S \dots \quad (6)$$

It should be noted that this transport equation is different from the usual transport equation encountered because the term  $(\vec{\nabla}_v \cdot \vec{a} + \partial v / \partial t)$  is generally nonzero as the bubble radius change rate,  $v(\vec{r}, \vec{v}, \ell, t)$ , and acceleration,  $\vec{a}(\vec{r}, \vec{v}, \ell, t)$ , are functions of bubble radius and bubble velocity respectively.

The distributed sources or sinks are contained in the term  $S \equiv S(\vec{r}, \vec{v}, \ell, t)$ . This term can also include the rate at which bubbles are introduced into  $d^7\tau$  and removed from  $d^7\tau$  by scattering off small scale turbulent eddies or by bubble-bubble interactions. It was assumed the  $S$  was independent of  $\psi$  or proportional to  $\psi$ . This simplification yielded a first order, partial differential bubble transport equation..



### III. FORMAL SOLUTION TO THE TRANSPORT EQUATION

The bubble transport Eq. (6) in the form of a first order partial differential equation was solved using the method of characteristics [Ref. 5]. This was equivalent to replacing the transport equation with a set of simultaneous, first order, ordinary differential equations.

The characteristic equations were determined to be the bubble dynamic equations:

$$\frac{d\vec{r}}{dt} = \vec{v} \quad \vec{r}(t_o) = \vec{r}_o = (x_o, y_o, z_o) \quad (7a)$$

$$\frac{d\vec{v}}{dt} = \vec{a} \quad \vec{v}(t_o) = \vec{v}_o = (v_{xo}, v_{yo}, v_{zo}) \quad (7b)$$

$$\frac{d\ell}{dt} = v \quad \ell(t_o) = \ell_o \quad (7c)$$

$$\frac{d\psi}{dt} = S - \sum_t \psi \quad \psi(t_o) = \psi_o \quad (7d)$$

The model chosen determined the acceleration  $\vec{a}(\vec{r}, \vec{v}, \ell, t)$  and rate of bubble radius change  $v(\vec{r}, \vec{v}, \ell, t)$ , thus establishing the family of characteristic curves. This family was parameterized by the set of initial conditions  $(\vec{r}_o, \vec{v}_o, \ell_o)$ , and  $\psi_o(\vec{r}_o, \vec{v}_o, \ell_o)$  was the initial distribution.

The general form of the distribution function was obtained by integrating Eq. (7d) and making use again of a Jacobian. The formal solution for the bubble distribution is [Ref. 5]:

$$\psi(\vec{r}, \vec{v}, \ell, t) d^7\tau = \psi(\vec{r}_o, \vec{v}_o, \ell_o, t) d^7\tau_o + \int_{t_o}^t S(\vec{r}^{\prime\prime}, \vec{v}^{\prime\prime}, \ell^{\prime\prime}, t^{\prime\prime}) d^7\tau^{\prime\prime} dt^{\prime\prime}$$

The integral here is a line integral along a characteristic curve as are all the integrals in this thesis. Equation (8) is equivalent to saying that the number of bubbles in  $d^7\tau$  about  $(\vec{r}, \vec{v}, \ell)$  at time  $t$  is the number of bubbles that were originally in  $d^7\tau_o$  plus or minus those added or subtracted by sources or sinks while proceeding along the characteristic curve.



#### IV. THE MODEL FOR THE SOLUTION OF THE BUBBLE TRANSPORT EQUATION

Before solutions to Eq. (6) could be obtained explicitly, a model of the upper ocean had to be specified. This model must provide explicit expressions for the acceleration  $\vec{a}(\vec{r}, \vec{v}, \ell, t)$ , the rate of change of bubble radius  $v(\vec{r}, \vec{v}, \ell, t)$ , the bubble distribution  $S(\vec{r}, \vec{v}, \ell, t)$  and the circulation field  $\vec{V}(\vec{r}, t)$ . A Cartesian coordinate system was chosen with the origin located at the surface of the ocean and the  $z$ -axis vertical and positive upward. Thus all depths were taken to be negative.

##### A. THE BUBBLE RADIUS CHANGE RATE

The rate of change of bubble radius for bubbles circulating in the ocean is caused by either gas diffusion, a change in the hydrostatic pressure, surface tension, or a combination of these phenomena. This interaction of effects was analyzed by assuming the bubbles to be spherical containing an ideal gas. From the ideal gas law

$$V = \frac{4}{3} \pi \ell^3 = \frac{nRT}{P} \quad (9)$$

where  $R$  is the gas constant,  $T$  is the temperature,  $P$  is the pressure, and  $V$  is the bubble volume. By taking the time derivative of Eq. (9) and assuming isothermal changes, an expression for  $v$ , the change in bubble radius was obtained:

$$v \equiv \frac{d\ell}{dt} = \frac{\ell}{3} \left[ \frac{1}{n} \frac{dn}{dt} - \frac{1}{P} \frac{dP}{dt} \right]. \quad (10)$$

The term  $\frac{1}{n} \frac{dn}{dt}$  contains the gas diffusion effects while the effects of the change in hydrostatic pressure and surface tension are contained in the term  $\frac{1}{P} \frac{dP}{dt}$ .



The hydrostatic pressure  $P$  is the sum of the atmospheric pressure,  $P_0$ , and the fluid pressure,  $-\rho_0 g z$ . The surface tension pressure is  $2\gamma/\ell$ , where  $\rho_0$  is the density of sea water,  $\rho_0 \approx 1.03 \times 10^3$  Kg/meter<sup>3</sup>, and  $\gamma$  is the surface tension of sea water, approximately equal to 0.74 newtons/meter. Therefore

$$P = P_0 - \rho_0 g z + 2\gamma/\ell \quad (11)$$

and

$$\frac{dP}{dt} = -\rho_0 g v_z - \frac{2\gamma}{\ell^2} \frac{d\ell}{dt}. \quad (12)$$

By using a simple model for gas diffusion [Ref. 8], the following expression was obtained for  $dn/dt$

$$\frac{dn}{dt} = -\delta 4\pi \ell^3 (P - P_0) \quad (13)$$

where  $\delta$  is a constant. A value for  $\delta$  had been determined from experimental data to be about  $10^{-6}$  meters/second. It was assumed for this model that the dissolved gas concentration gradient was confined to a thin shell at the air-water boundary because of the bubble's speed.

An expression for  $v$  was obtained by substituting Eqs. (11), (12), and (13) into Eq. (10) [Ref. 5].

$$v \equiv \frac{d\ell}{dt} = [v_z \ell^2 + 3\delta RT(z\ell - \Gamma)]/[3(D-z)\ell + 2\Gamma] \quad (14)$$

where

$$\Gamma \equiv 2\gamma/\rho_0 g \approx 1.47 \times 10^{-5} \text{ meters}^2$$

and

$$D \equiv P_0/\rho_0 g \approx 10 \text{ meters}.$$

If  $\ell$  is greater than 30 microns (1 micron ( $\mu$ ) =  $10^{-6}$  meters), the surface tension terms can be ignored, i.e.,  $\Gamma = 0$ .



## B. THE BUBBLE EQUATION OF MOTION AND ACCELERATION

A bubble that is in motion with respect to a stationary reference system will experience several forces acting on it. First there is the force of the water acting on the bubble to pull it along. If the bubble were completely entrained by the fluid so that the bubble's velocity ( $\vec{v}$ ) were equal to the circulation field velocity ( $\vec{V}$ ), the entrainment force would be  $\rho_0 \sigma d\vec{V}/dt$  where  $\sigma$  is the volume of the bubble. Complete entrainment can occur only if  $\rho$  is equal to  $\rho_0$ . Since this is rarely the case, the bubble will maintain a relative velocity  $\vec{u} = \vec{v} - \vec{V}$  with respect to the water. This relative velocity produces a drag force,  $\vec{F}_D$ , acting on the bubble to slow it down.

As the bubble moves through the water, the bubble pulls water along with it. The amount of water pulled along with it is equal to some fraction,  $\beta$ , of the bubble's volume. From experimental data  $\beta$  is usually taken as 0.5. This phenomena is called the mass adhering force and is equal to  $-(\beta \sigma \rho_0 d\vec{u}/dt)$ . The bubble will also experience a net buoyant force which is equal to  $\sigma g(\rho_0 - \rho) \hat{z}$ , where  $g$  is the gravitational acceleration.

By using Newton's second law these forces were combined to yield an expression for the acceleration  $\vec{a}$  [Ref. 5]:

$$\vec{a} = \frac{\vec{F}_D}{\sigma \rho_0 (\beta + \rho/\rho_0)} + \frac{1+\beta}{(\beta + \rho/\rho_0)} \frac{d\vec{V}}{dt} + \frac{(1-\rho/\rho_0)}{(\beta + \rho/\rho_0)} g \hat{z} \quad (15)$$

where

$$\frac{d\vec{V}}{dt} = \frac{\partial \vec{V}}{\partial t} + (\vec{v} \cdot \vec{\nabla}) \vec{V} \quad (16)$$

In order to obtain an explicit expression for the acceleration  $\vec{a}$ , it was necessary to derive an expression for the drag force  $\vec{F}_D$ . Various



models for the drag force were considered, with the models being classified by using the Reynold's number  $R_e = 2\ell\mu\rho_o/\eta$  where  $\eta$  is the viscosity of water ( $\eta \approx 10^{-3}$  Newton-second/meter<sup>2</sup>).

For bubbles with a radius less than or equal to 100 microns ( $\ell \leq 100$ ), the Reynold's number is less than one ( $R_e \ll 1$ ) and the drag is viscous according to Stokes Law:

$$\vec{F}_D = \vec{F}_{\text{Stokes}} = -K\eta\vec{u} \quad (17)$$

where  $K = 6\pi$  in the presence of surface active material and  $4\pi$  in the absence of these surface active materials..

The drag was considered to be both viscous and turbulent if  $100\mu \leq \ell \leq 1500\mu$  or  $1 \leq R_e \leq 700$ . Thus the drag force was

$$\vec{F}_D = \vec{F}_{\text{Stokes}} + \vec{F}_{\text{Turb}} \quad (18)$$

Here  $\vec{F}_{\text{Stokes}}$  was given as in Eq. (17) with  $6\pi \leq K \leq 12\pi$  and  $\vec{F}_{\text{Turb}}$ , which arise from the energy dissipated in the turbulence of the wake, had the form:

$$\vec{F}_{\text{Turb}} = -0.5 K_f \rho_o s_1 \vec{u} \vec{u} \quad (19)$$

where  $K_f$  is a drag coefficient and  $s_1$  is the bubble surface area covered by the turbulent wake ( $s_1 = \pi\ell^2$ ). If there were no surface active materials present  $\vec{F}_D$  would equal  $\vec{F}_{\text{Stokes}}$ , with  $K = 12\pi$ .

Since the oceans contain surface active materials, the drag force contains both a viscous drag and turbulent drag term. By noting that  $\rho/\rho_o \ll 1$  and that  $\sigma = 4\pi\ell^3/3$  for bubbles with  $\ell < 1500\mu$ , the acceleration can be written as [Ref. 5]:

$$\vec{a} = -\left(\frac{\alpha}{\ell^2}\right)\vec{u} - \left(\frac{\xi}{\ell}\right)\vec{u}\vec{u} + \left(\frac{\xi}{\beta}\right)\hat{z} + \left(1 + \frac{1}{\beta}\right)d\vec{V}/dt \quad (20)$$



with

$$\alpha = \frac{9}{2} \frac{\eta}{\beta \rho_0} = 8.75 \times 10^{-6} \text{ meters/sec}^2$$

and

$$\xi = \frac{3}{2} \frac{K_F}{\beta} \frac{s_1}{4\pi l^2} = 4.5 \times 10^{-1} ..$$

If the bubbles were generated by a surface source such as rain, wave action, etc., the bubble radii are generally less than  $150 \mu$  [Refs. 3 and 9] and the drag force is predominately viscous.. In this case  $\xi$  should be set equal to zero..

If the bubbles originate at a bottom source, the radii are in the range of  $500 \mu$  to  $700 \mu$  [Ref. 4] and the drag should be considered to be predominately turbulent with  $\alpha$  set equal to zero..

### C. BUBBLE SOURCES

The bubbles in the ocean might physically be considered to have originated from three types of sources.. The first type included bubbles that originated near the surface and were caused by wave action, rain or snow. The distribution of bubbles originating from these phenomena was analyzed in Ref. 10..

The second type of bubbles are those nucleated by distributed particles of material as well as bubbles that originated from biological activity such as photosynthesis or bacteria and are distributed throughout the medium.

The third type of bubbles includes those bubbles generated on the floor of the ocean. These bubbles are often sediment-initiated bubbles and measurements indicate these bubbles to be between  $450 \mu$  --  $800 \mu$  in radius with a peak around  $550 \mu$  [Ref. 4]. It was this category of bubbles for which the distribution function was evaluated. It was



considered to be mathematically convenient to introduce the bubbles via boundary conditions rather than to include them in  $S(\vec{r}, \vec{v}, \ell, t)$ .  $\psi_o(\vec{r}_o, \vec{v}_o, \ell_o)$  represented the bubble distribution originating in the bottom sediment.

The model for the circulation field was chosen to be a quiescent fluid dictating that  $\vec{V} = 0$ . For this model the bubbles could rise only via buoyancy and the characteristic curves are vertical upward.



## V. RESULTS

For this thesis the bubble transport theory was applied to a one-dimensional quiescent, steady state ocean with a bottom source at 197 meters. The solution and approximate solutions are given. The characteristic equations were integrated numerically to test the accuracy of the approximate analytical solutions. The calculated bubble distributions were compared with experimental data.

In this steady state model the velocities are vertical upward, and all functions depend spatially on depth only. The bubble transport equation (Eq. 6) can be written as:

$$v \frac{d\phi}{dz} + a \frac{d\phi}{dv} + v \frac{d\phi}{dl} = - \Sigma_t \phi + S. \quad (21)$$

Here  $\phi(z, v, l)$  is the distribution function,  $S$  is the distributed source function,  $v$  is the vertical velocity,  $v$  is the rate of change of bubble radius, and  $\Sigma_t \equiv \partial a / \partial v + \partial v / \partial l$ .

If  $z$  is chosen as the independent parameter, the characteristic equations are [Ref. 5]:

$$\frac{dv}{dz} = \frac{a}{v} = - \frac{\alpha}{l^2} - \frac{\xi}{l} v + \frac{g}{\beta v} \quad (22a)$$

$$\frac{dl}{dz} = \frac{v}{l} = \frac{l^2 + 3\xi RT(zl - \Gamma)/v}{3(D-z)l + 2\Gamma} \quad (22b)$$

and

$$\frac{d\phi}{dz} = - \frac{1}{v} \Sigma_t \phi + \frac{I}{v} S. \quad (22c)$$

Since the characteristic curves are vertically upward along the  $z$ -axis, the characteristics or boundary conditions are  $v = v_o$ ,  $l = l_o$ , and  $\phi = \phi(z_o, v_o, l_o)$  at  $z = z_o \leq 0$ .



Equation (22c) was integrated to yield

$$\begin{aligned}\phi(z, v, \ell) = & \phi(z_0, v_0, \ell_0) \exp \left[ - \int_{z_0}^z \Sigma_t(z', v', \ell') dz' / v' \right] \\ & + \int_{z_0}^z \exp \left[ - \int_{z'}^z \Sigma_t(z'', v'', \ell'') dz'' / v'' \right] S(z', v', \ell') dz' / v' \quad (23)\end{aligned}$$

with the integration taking place along the characteristic curves

$\{z, v(z; z_0, v_0, \ell_0), \ell(z; z_0, v_0, \ell_0); z \leq 0\}$ . By using the Jacobian Eq. (23) was rewritten as [Ref. 5]:

$$\begin{aligned}v\phi(z, v, \ell) dv d\ell = & v_0 \phi(z_0, v_0, \ell_0) dv_0 d\ell_0 \\ & + \int_{z_0}^z S(z', v', \ell') dz' dv' d\ell'. \quad (24)\end{aligned}$$

Equation (24) is interpreted as a conservation equation which states that the flux of bubbles,  $v\phi$ , at the point  $(z, v, \ell)$  is equal to the flux of bubbles,  $v_0\phi_0$ , at the point  $(z_0, v_0, \ell_0)$  plus (or minus) any bubbles added (or subtracted) by distributed sources along the characteristic curve.

Prior to the calculation of the distribution function in either Eq. (23) or Eq. (24) it was necessary to establish a mapping between points  $(z, v, \ell)$  and  $(z', v', \ell')$  on the characteristic curve. This was done by integrating simultaneously the characteristic equations (Eq. 22) to obtain  $v(z, \ell; z', v', \ell')$  and  $\ell(z, \ell; z', v', \ell')$  for various  $z', v'$ , and  $\ell'$  and substituting these relationships into Eq. (23). Since  $\alpha/\ell^2 \gg 1$ , it was very time consuming to integrate Eq. (22a) numerically. Referring to Fig. 1, it is seen that an appropriate approximation is to equate the velocity and the terminal velocity. This permits semi-analytical solutions.



This approximation can be verified by rewriting Eq. (22a) as

[Ref. 5]

$$\frac{dv}{dz} = - \left( \frac{\xi}{\ell} \right) (v - v_T) (v + v'_T) \quad (25)$$

where

$$v_T = \frac{-1 + [1 + 4(v_{T1}/v_{T2})^2]^{1/2}}{2(v_{T1}/v_{T2})} \quad (26)$$

and

$$v'_T = \frac{1 + [1 + 4(v_{T1}/v_{T2})^2]^{1/2}}{2(v_{T1}/v_{T2})} \quad (27)$$

$$v_{T1} = \left[ \frac{g}{\beta} \frac{\ell^2}{\alpha} \right]^{1/2} \quad (28a)$$

is the terminal velocity in the case where viscous drag dominates ( $\ell \leq 100 \mu$ ).

$$v_{T2} = \left[ \frac{g}{\beta} \frac{\ell}{\xi} \right]^{1/2} \quad (28b)$$

is the terminal velocity in the case where turbulent drag dominates ( $\ell \geq 400 \mu$ ). Thus

$$v_T = \begin{cases} v_{T1} & \text{for } \ell \leq 100 \\ v_{T2} & \text{for } \ell \geq 400 \end{cases} \quad (29)$$

Equation (25) was integrated using fourth rank optional Runge Kutta [Ref. 11]. These numerical results are presented graphically in Fig. 1. It is observed that when a bubble is released from a depth of 20.00 meters with zero velocity, it will reach terminal velocity after having traveled a distance of only several bubble radii. Thus the approximation that  $v = v_T$  is considered to be a valid approximation for this model. This approximation is convenient as Eq. (22a) is very difficult to integrate numerically.



By using the approximation  $v = v_T$ , the bubble distribution function can be written approximately as:

$$\phi(z, v, \ell) = \delta(v - v_T) \Phi(z, \ell) \quad (30)$$

where

$$\Phi(z, \ell) = \int_{-\infty}^{\infty} \phi(z, v, \ell) dv \quad (31)$$

is the "depth-radius" distribution function. By substituting Eq. (31) into Eq. (24) and integrating over  $v$ , an expression for  $\Phi$  was determined as [Ref. 5]:

$$\Phi(z, \ell) = \frac{v_{T0}}{v_T} \Phi(z_0, \ell_0) \left( \frac{\partial \ell_0}{\partial \ell} \right) + \frac{I}{v_T} \int_{z_0}^z s(z', \ell') \left( \frac{\partial \ell'}{\partial \ell} \right) dz' \quad (32)$$

where

$$s(z', \ell') \equiv \int_{-\infty}^{\infty} S(z'', v'', \ell'') dv'' \quad (33a)$$

and

$$d\ell_0 = \left( \frac{\partial \ell_0}{\partial \ell} \right) d\ell, \text{ etc.} \quad (33b)$$

In order to calculate  $\Phi(z, \ell)$ , it was necessary to determine  $\partial \ell' / \partial \ell$  and  $\ell'(z'; z, \ell)$  either analytically or numerically. Note that  $\partial \ell' / \partial \ell = 1 / (\partial \ell / \partial \ell')$ , and that the approximate differential equation that  $\partial \ell / \partial \ell'$  satisfies is obtained by setting  $v = v_T$  in Eq. (22b) and taking the partial derivative with respect to  $\ell'$  [Ref. 5]:

$$\frac{\partial}{\partial z} \frac{\partial \ell}{\partial \ell'} = \left\{ \left( \frac{2\Gamma}{\ell^2} \right) \left[ \ell - \left( \frac{3\delta RT}{v_T} \right) \left( \frac{\Gamma}{\ell} - z \right) \right] \right/ \left[ 3(D-z) + \frac{2\Gamma}{\ell} \right] + \left[ 1 + \left( \frac{3\delta RT}{v_T} \right) \left[ \frac{\Gamma}{\ell^2} + \left( \frac{\Gamma}{\ell} - z \right) \left( \frac{\partial v_T}{\partial \ell} \right) \right] \right] \right\} \right/ \left[ 3(D-z) + \frac{2\Gamma}{\ell} \right], \quad (34a)$$

where

$$\frac{\partial v_T}{\partial \ell} = \frac{3v_{T1}}{\ell} \left[ 1 + 4 \left( \frac{v_{T1}}{v_{T2}} \right)^2 \right]^{-1/2} - \frac{v_T}{\ell}. \quad (34b)$$

Furthermore, with the approximation  $v = v_T$ , then  $\ell = \ell_T$ , and Eq. (22b)



becomes

$$\frac{d\ell_T}{dz} = \frac{\ell^2 + 3\delta RT(z\ell - \Gamma)/v_T}{3(D-z)\ell + 2\Gamma} \quad (35)$$

Equations (34) and (35) can be integrated numerically using optimal fourth rank Runge Kutta [Ref. 11]. These results can be substituted into Eq. (32) to obtain  $\Phi = \Phi_T$  for various sources. Since  $v = v_T$  is a good approximation, it is expected that the approximation  $\ell = \ell_T$  will also be very good.

To obtain approximate analytical results for comparison to the more exact numerical results outlined above, the approximations of Eq. (29) can be used. Neglecting surface tension,  $\Gamma = 0$  is also a valid approximation for  $\ell \geq 30 \mu$ . Then Eq. (35) can be integrated analytically [Ref. 5]. For  $v = v_{T1}$  and  $\Gamma = 0$

$$\ell = \ell_{T1}(z; z', \ell') = \left[ \frac{D-z}{D-z'} \ell'^3 + \frac{3}{2} \frac{\alpha \delta RT}{(g/\beta)} \frac{z^2 z'^2}{D-z'} \right]^{1/3} \quad (36a)$$

For  $v = v_{T2}$  and  $\Gamma = 0$

$$\ell = \ell_{T2}(z, z', \ell') = \left\{ \left( \frac{D-z'}{D-z} \right)^{1/2} \ell'^{3/2} + \frac{\delta RT}{((g/\beta)\xi)^{1/2}} \left[ (D-z) \left( 1 - \left( \frac{D-z'}{D-z} \right)^{3/2} \right) - 3D \left( 1 - \left( \frac{D-z'}{D-z} \right)^{1/2} \right) \right] \right\}^{2/3} \quad (37a)$$

The inverse transformation are

$$\ell = \ell_{T1}(z'; z, \ell) \quad (36b)$$

and

$$\ell = \ell_{T2}(z'; z, \ell) \quad (37b)$$

respectively. Then

$$\frac{\partial \ell'}{\partial \ell} = \left( \frac{D-z}{D-z'} \right) \frac{\ell^2}{\ell'^2} \quad (36c)$$



and

$$\frac{\partial \ell'}{\partial \ell} = \left( \frac{D-z}{D-z'} \right)^{1/2} \left( \frac{\ell}{\ell'} \right)^{1/2} \quad (37c)$$

respectively. If gas diffusion can be neglected,  $\delta = 0$ , then Eqs. (36) and (37) reduce to:

$$\frac{\ell}{\ell'} = \left( \frac{D-z'}{D-z} \right)^{1/3} \quad (38a)$$

$$\frac{\partial \ell'}{\partial \ell} = \left( \frac{D-z}{D-z'} \right)^{1/3} \quad (38b)$$

Figures (2), (3), (4), (5), and (6) demonstrate the results obtained by integrating Eq. (35) numerically and comparing  $\ell_T$  to the analytical approximations of Eqs. (36), (37), and (38). Figures (2), (3), and (4) were drawn for a depth of 20 meters and Figs. (5) and (6) were drawn for a depth of 197 meters. Figures (2) and (5) demonstrate that  $\ell_{T1}$  is a good approximation for  $\ell_T$  when  $\ell \leq 100 \mu$ . However, this approximation breaks down when  $\ell < 30 \mu$ . This is because the effects of surface tension, which are important in bubbles of  $\ell \leq 30 \mu$ , are neglected. Figures (3), (4), and (6) demonstrate that  $\ell_{T2}$  is a good approximation for  $\ell_T$  when  $\ell \geq 400 \mu$ . From Fig. (6), it is observed that  $\ell_{T3}$  is not a good approximation for  $\ell$ . This is because  $\ell_{T3}$  neglects the effects of gas diffusion.

The survival threshold for bubbles is different depending on whether the bubbles were released at a depth 20 meters or 197 meters. In the 20 meter case, bubbles of  $\ell \geq 100 \mu$  will reach the surface, while in the 197 meter case, bubbles of  $\ell \geq 1000$  meters will surface. This difference is caused by gas diffusion being dominate over the decrease in hydrostatic pressure. Since gas diffusion is proportional to  $(P-P_0)/P$ , it will be constant for  $z \leq 30$  meters and will only



decrease for  $z \geq 30$  meters. Thus bubbles released at 197 meters are exposed to a high gas diffusion rate for practically all their travel, while bubbles released at 20 meters are exposed to a decreasing gas diffusion rate.

Finally the bubble distribution function was calculated for each of these approximate solutions to Eqs. (22a) and (22b), (34) and (35), (36), (37), and (38). It was convenient to introduce the initial distribution function as the boundary condition  $\Phi(z; z_o, \ell_o)$  instead of as a distributed source. Since  $s(z', \ell')$  is zero, the solution can be written as

$$\Phi(z; z_o, \ell_o) = \frac{V_{T_o}}{V_T} \Phi(z_o, \ell_o) 1/(\partial \ell / \partial \ell'). \quad (39a)$$

For  $v = v_T$ , Eqs. (34) and (35) must be integrated numerically to yield  $\Phi_T(z; z_o, \ell_o)$ . For  $v = v_{T1}$  ( $\ell \leq 100\mu$ ) and  $\Gamma = 0$

$$\Phi \approx \Phi_1(z; z_o, \ell_o) = \left( \frac{D-z}{D-z_o} \right) \Phi(z_o, \ell_o); \quad (39b)$$

for  $v = v_{T2}$  ( $\ell \geq 400\mu$ )

$$\Phi \approx \Phi_2(z; z_o, \ell_o) = \left( \frac{D-z}{D-z_o} \right)^{1/2} \Phi(z_o, \ell_o); \quad (39c)$$

and if the effects of gas diffusion are not considered

$$\Phi \approx \Phi_3(z; z_o, \ell_o) = \frac{V_{T_o}}{V_T} \Phi(z_o, \ell_o) \left( \frac{D-z}{D-z_o} \right)^{1/3} \quad (39d)$$

Here  $V_{T3}$  is computed using

$$\ell = \ell_o \left( \frac{D-z}{D-z_o} \right)^{1/3}$$

in Eq. (26).

The above distributions were calculated using an initial distribution function,  $\Phi(z_o, \ell_o)$ , obtained from Ref. 4. The authors of Ref. 4



determined the distribution of bubbles rising from "the highly organic, anaerobic sediment on the bottom" of Saanich Inlet, British Columbia. The depth of the water was 197 meters. The density of these rising bubbles was determined by using stationary echo-sounders operating at various frequencies in the kilohertz range. Figure 7a is a histogram that presents the presumed bubble distribution,  $\Phi(z_o, l_o)$  at a depth of 197 meters as presented in Ref. 4. Figures (7b) through (7g) demonstrate how this initial distribution changes as the bubbles rise in height. It should be noted that height is measured from the ocean bottom upward to the surface.

The different histograms at each height above the ocean floor shows how the bubble distribution is changing depending on the model chosen to be used for the calculation of  $l_T$ . In the model where gas diffusion as well as hydrostatic pressure changes are considered, the bubble distribution  $\Phi(z; z_o, l_o)$  shifts toward smaller size bubbles as height increases. It can also be observed that the width of the intervals is increasing with height. Finally all the bubbles disappear entirely at a height of about 100 meters.

In the small bubble approximation  $\Phi \approx \Phi_1(z; z_o, l_o)$ , where the drag force is considered to be viscous and  $v = v_{T1}$ , the bubble distribution appears to spread out by shifting toward bubbles of both smaller and larger radii. Bubbles with initial radius less than 900  $\mu$  continually decrease in radius, while bubbles with an initial radius greater than 900  $\mu$  will initially decrease in size but as the effects of gas diffusion reduce, these bubbles expand. In the turbulent drag model,  $v = v_{T2}$ ,  $\Phi = \Phi_2(z; z_o, l_o)$  shifts toward smaller radius bubbles because of the effect of gas diffusion and disappears at a height of about 125 meters.



When gas diffusion is neglected, the bubble distribution

$\phi \approx \phi_3(z; z_o, l_o)$  shifts toward bubbles of larger radii. This was to be expected because as hydrostatic pressure decreased, the bubbles would increase in size. The bubble distribution calculated for  $\phi_3(z; z_o, l_o)$  compares quite well with the experimental data of McCartney and Bary in Ref. 4. It appears as though gas diffusion was somehow not important in the bubbles they measured. These bubbles originated at the bottom, so perhaps they had some kind of coating that impeded gas diffusion across their surfaces.



## VI. CONCLUSION

Calculating bubble distributions in the ocean by solving the bubble transport equation appeared to be quite feasible. Although the solution of the transport equation can be quite involved, a careful choice of approximations often permits approximate analytical solutions. Otherwise, the equations can usually be numerically integrated. For the model chosen, analytical expressions were obtained for several approximations. All of these expressions yielded results that were in general agreement with experimental data or with intuitive reasoning. It was seen that the drag force model chosen and the inclusion of gas diffusion greatly influenced the results obtained.

The assumption that the velocity of the bubble was equal to the terminal velocity should be quite valid as the data presented on Fig. 1 demonstrated. With this approximation, one can easily calculate the bubble radius at any depth. The radius is strongly dependent on the model chosen for the drag force, gas diffusion and surface tension. The choice of the drag model determines the equation used to calculate the terminal velocity.

Finally the distribution function for a bottom source was calculated. The data generated by this theoretical approach agrees well with the limited experimental data available. The distribution calculated for the no gas diffusion model yields data that is in good agreement with the experimental data in Ref. 4.

From the limited amount of experimental data available, it appears that gas diffusion is unimportant in bubbles originating in bottom



sediment and transported to the surface. It is felt that the type of gas in the bubbles would greatly influence the amount of diffusion that would take place [Ref. 12]. Since a fluid, super-saturated with the same gas that is within the bubble, is the only fluid in which gas diffusion is not considered the dominating effect, there must be some mechanism inhibiting gas diffusion from sediment bubbles.. Further investigation into this phenomena seems warranted.



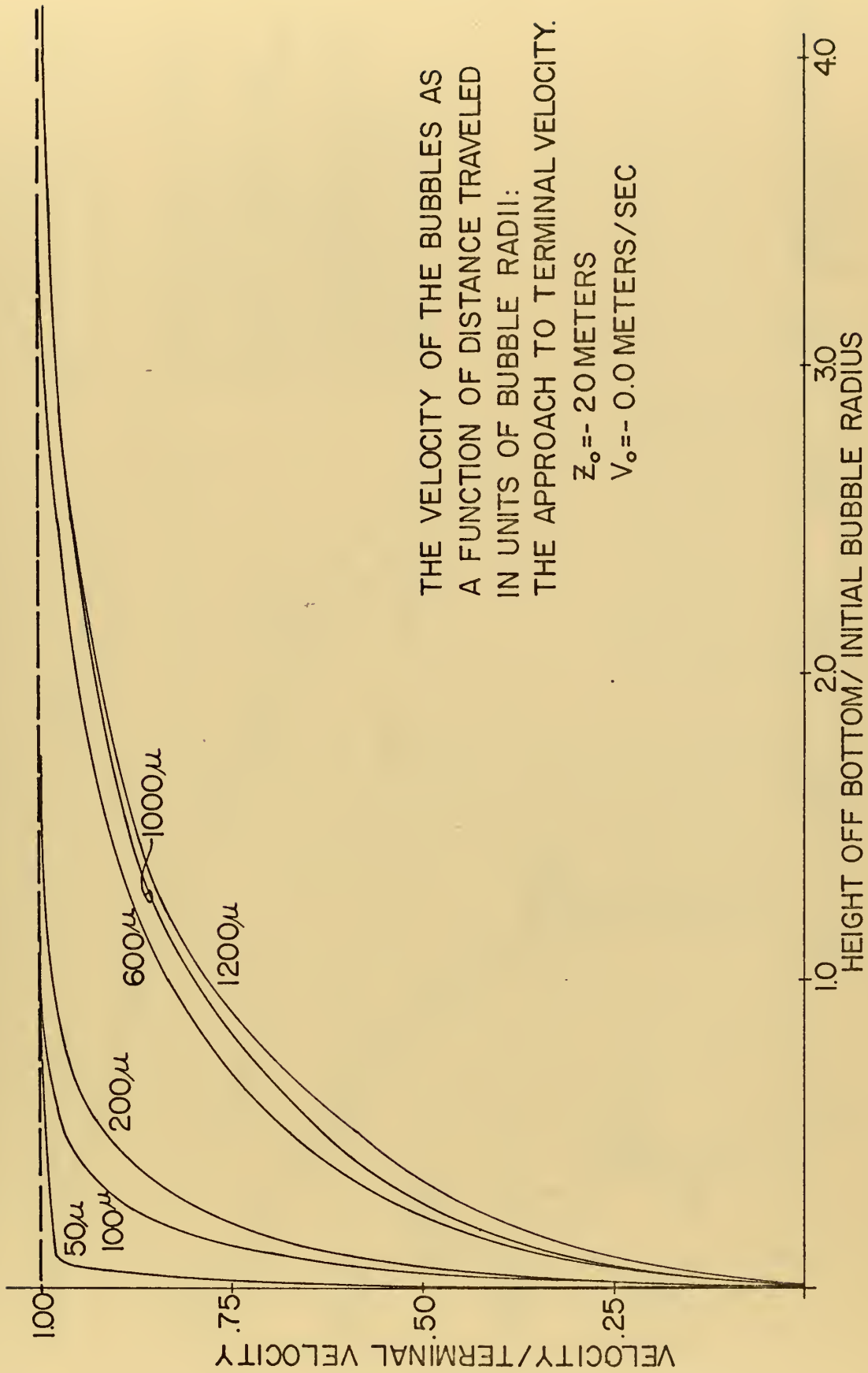


Figure 1



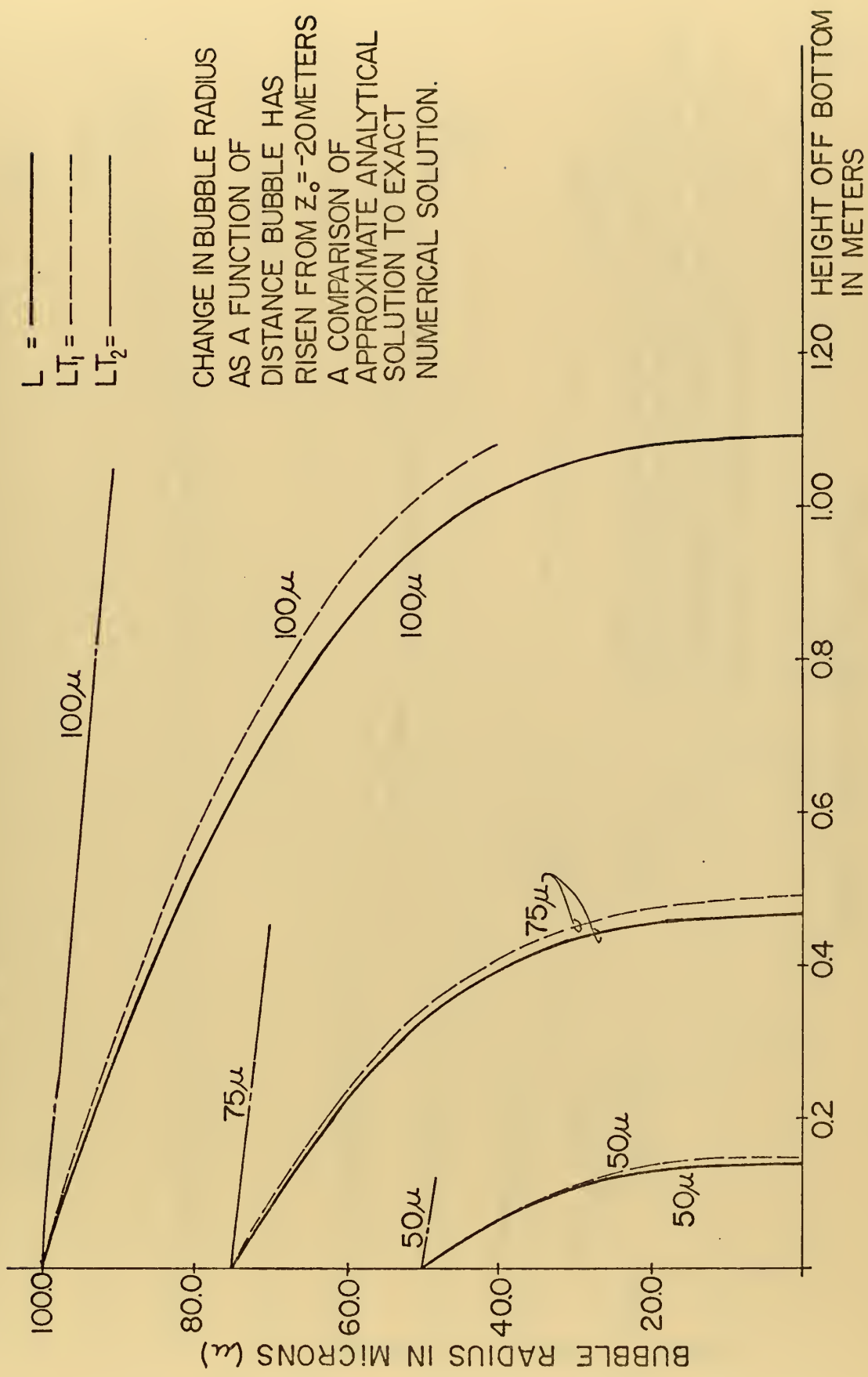


Figure 2



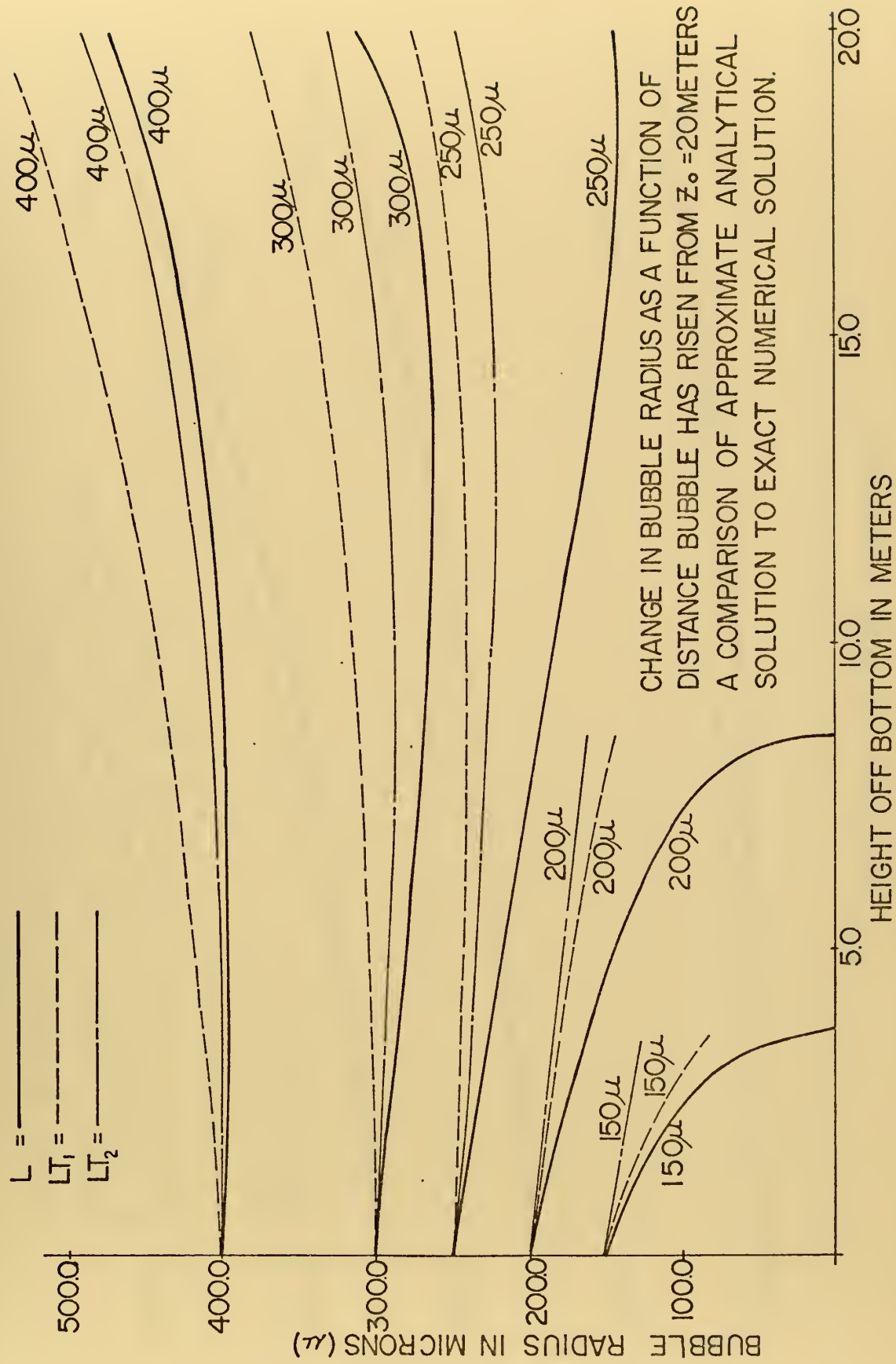


Figure 2



CHANGE IN BUBBLE RADIUS AS A FUNCTION OF  
 DISTANCE BUBBLE HAS RISEN FROM  $z_0 = 20$  METERS  
 A COMPARISON OF APPROXIMATE ANALYTICAL  
 SOLUTION TO EXACT NUMERICAL SOLUTION.

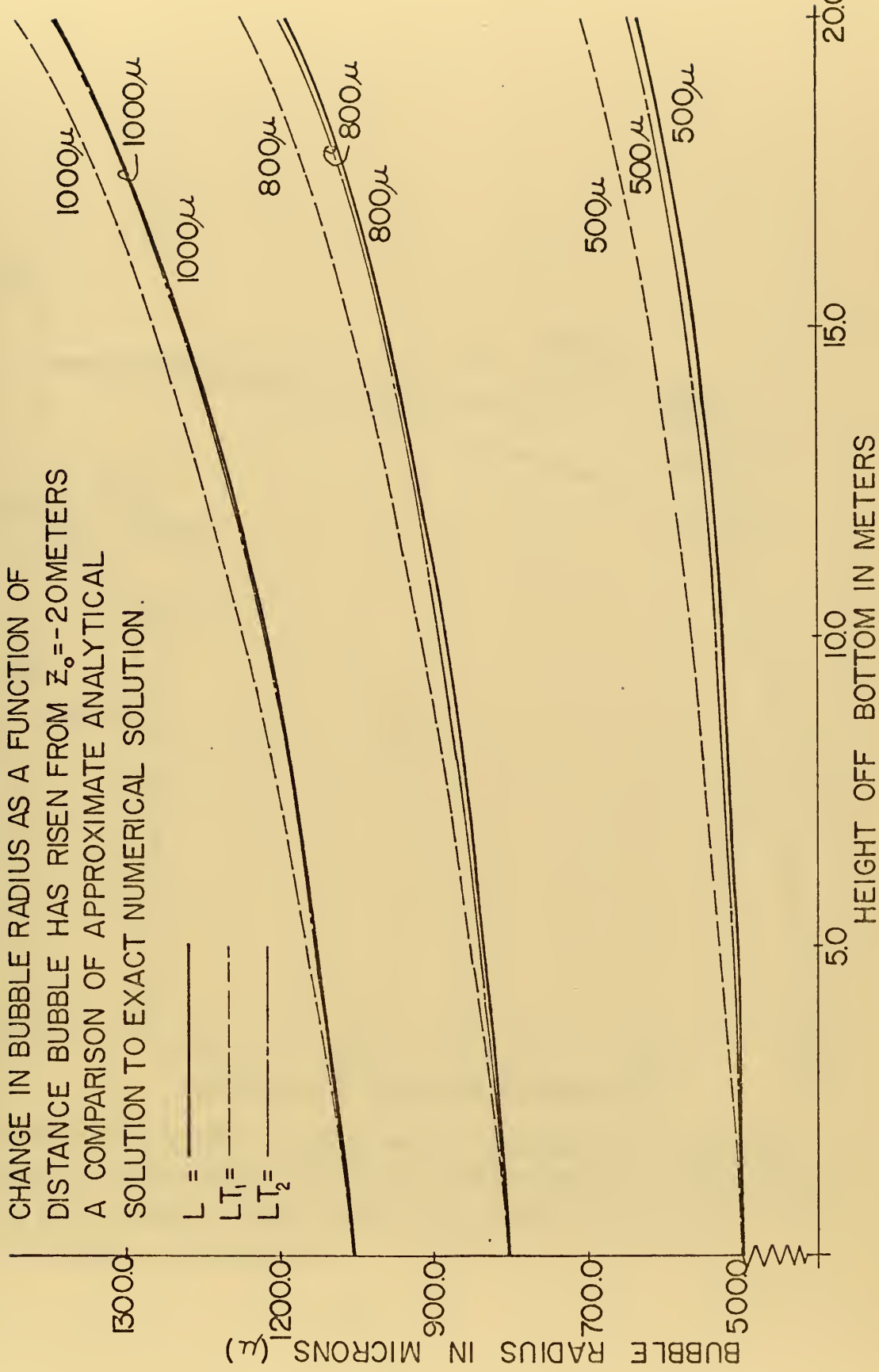
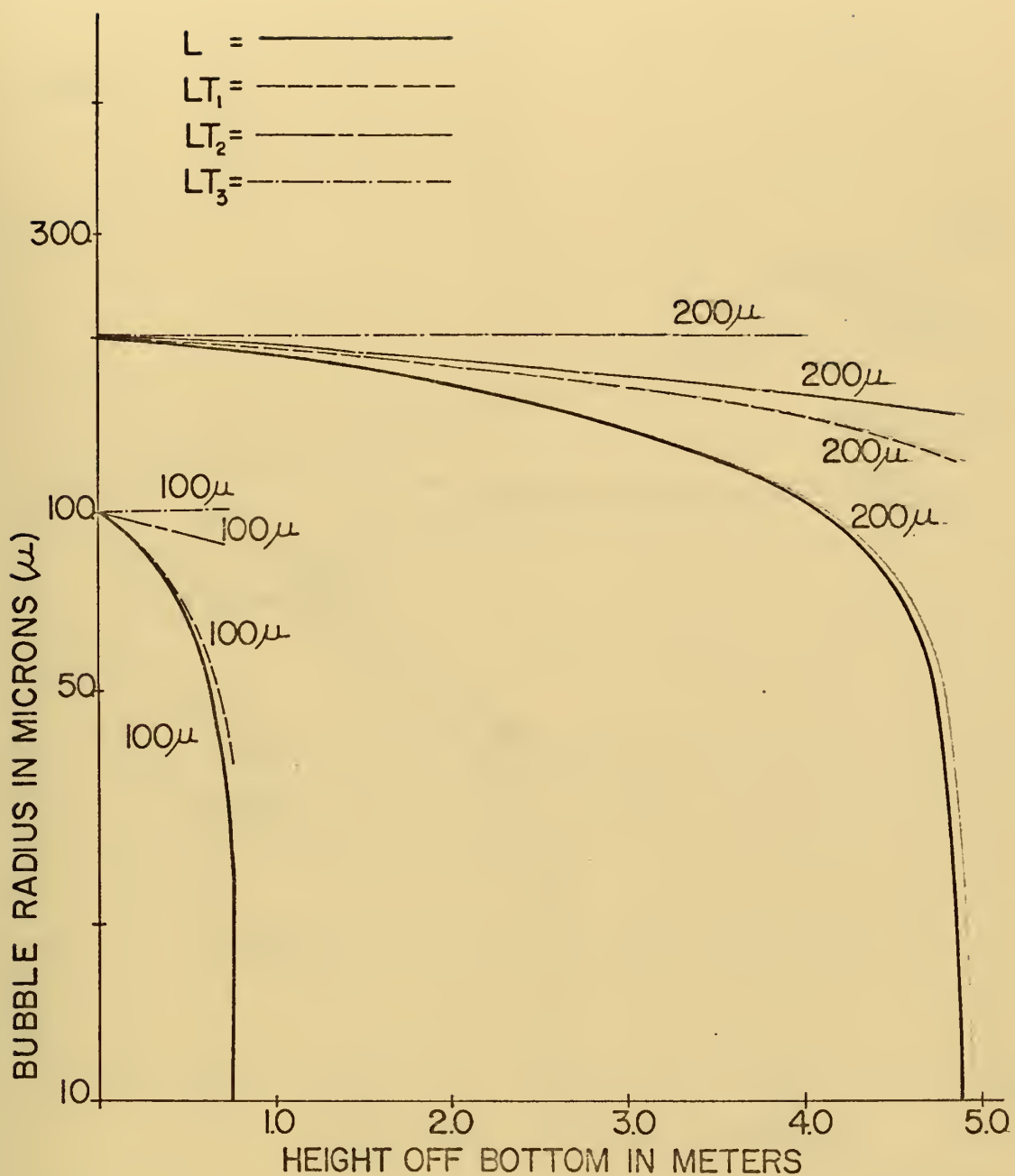


Figure 4

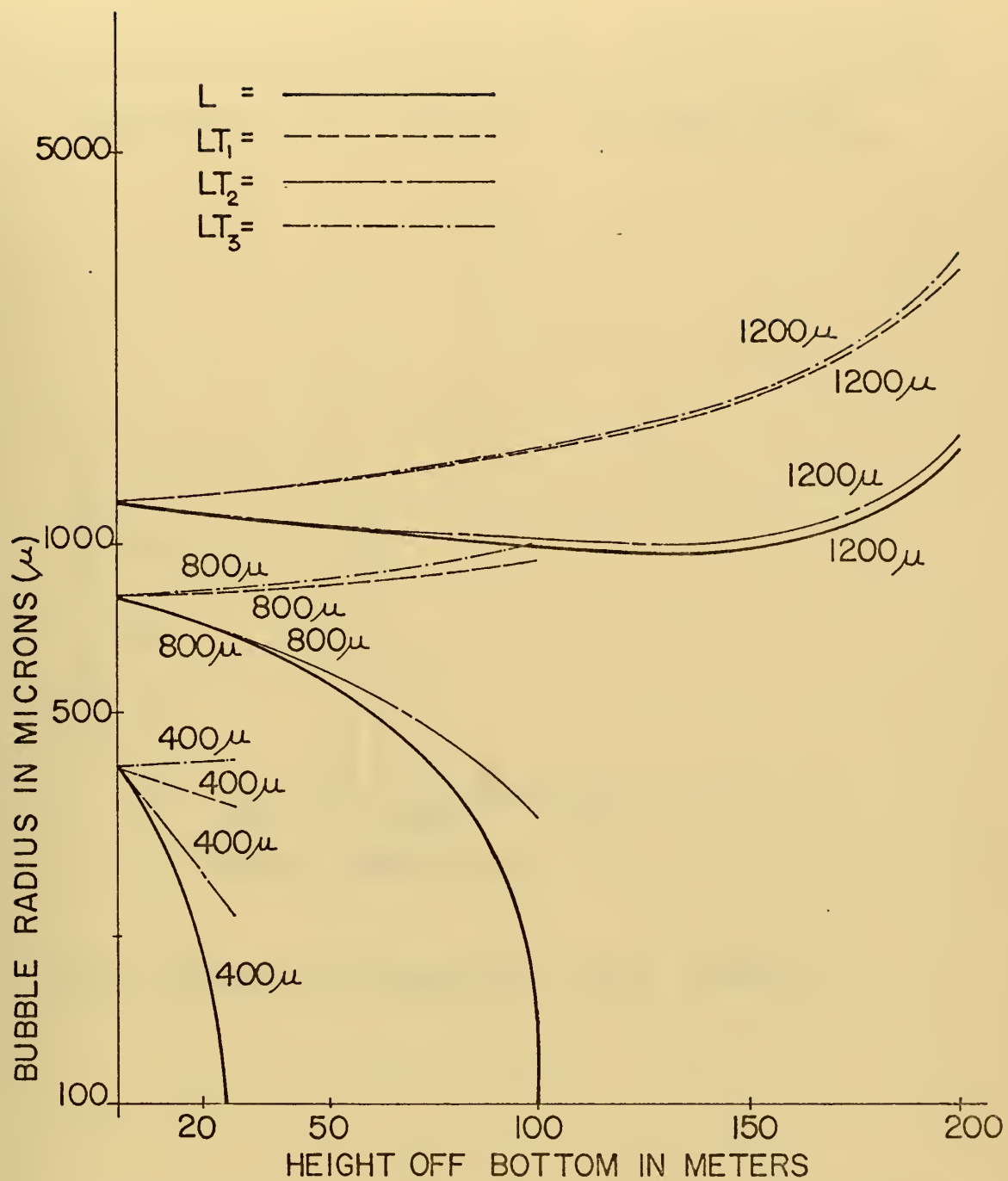




CHANGE IN BUBBLE RADIUS AS A FUNCTION OF DISTANCE  
 BUBBLE HAS RISEN FROM  $z_0 = -197$  METERS A COMPARISON  
 OF APPROXIMATE ANALYTICAL SOLUTION TO EXACT  
 NUMERICAL SOLUTION.

Figure 5



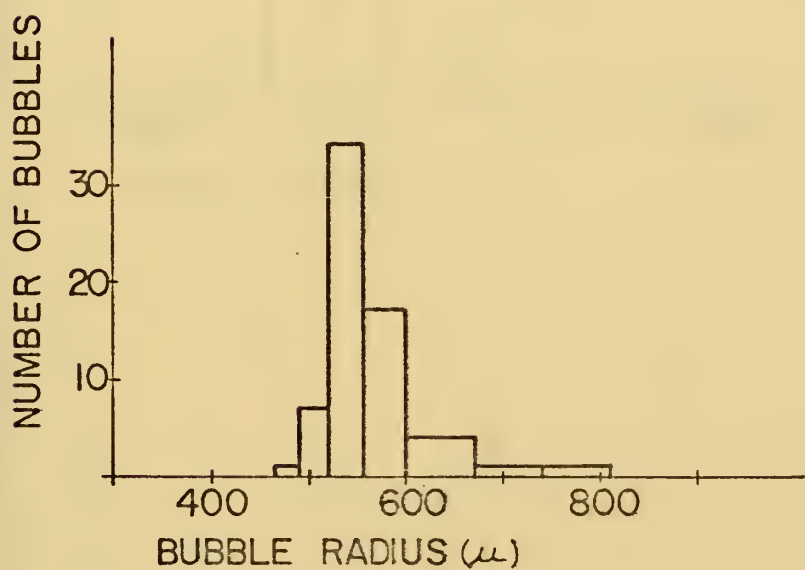


CHANGE IN BUBBLE RADIUS AS A FUNCTION OF DISTANCE  
 BUBBLE HAS RISEN FROM  $z_0 = -197$  METERS A COMPARISON  
 OF APPROXIMATE ANALYTICAL SOLUTION TO EXACT  
 NUMERICAL SOLUTION.

Figure 6



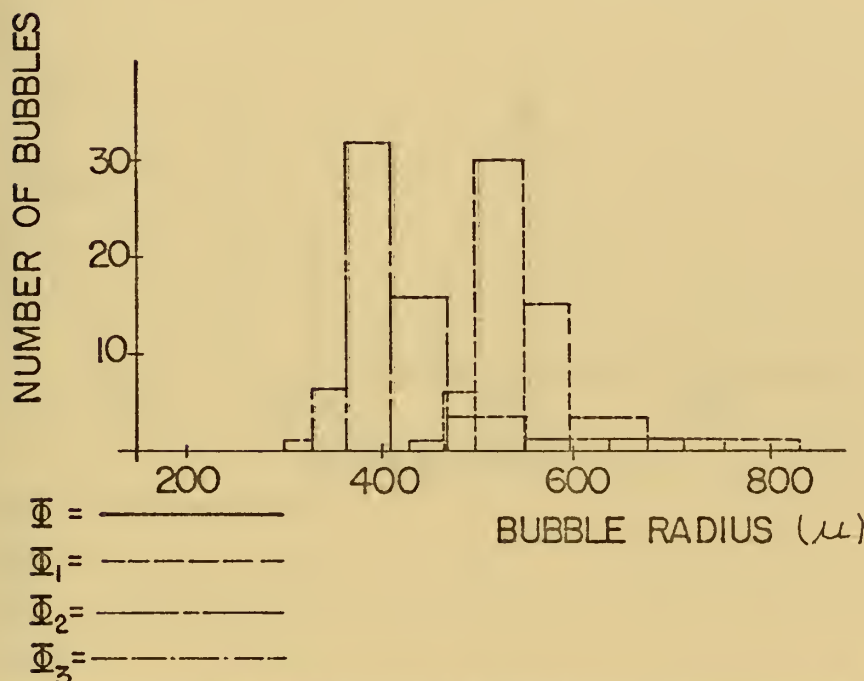
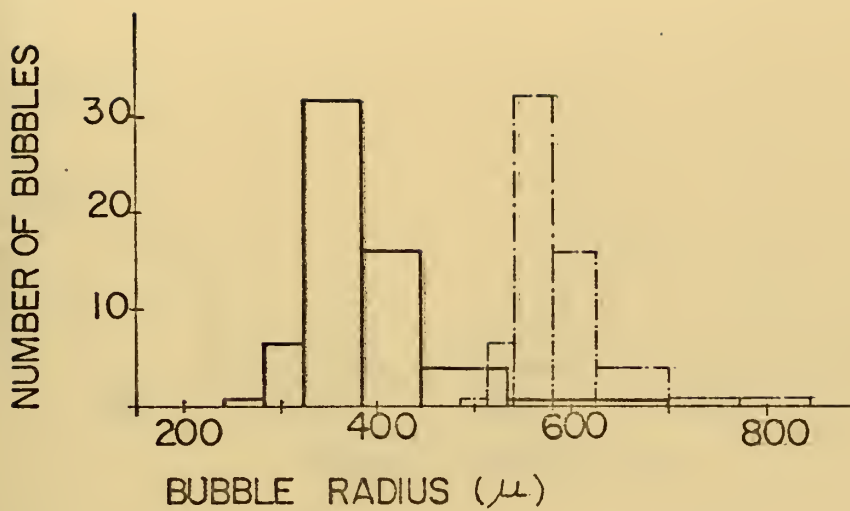
DISTRIBUTION OF BUBBLES ORIGINATING IN  
SEDIMENT AT DEPTH 197 METERS.



INITIAL BUBBLE DISTRIBUTION  $\xi(z, l)$  (REF. 4)

Figure 7a

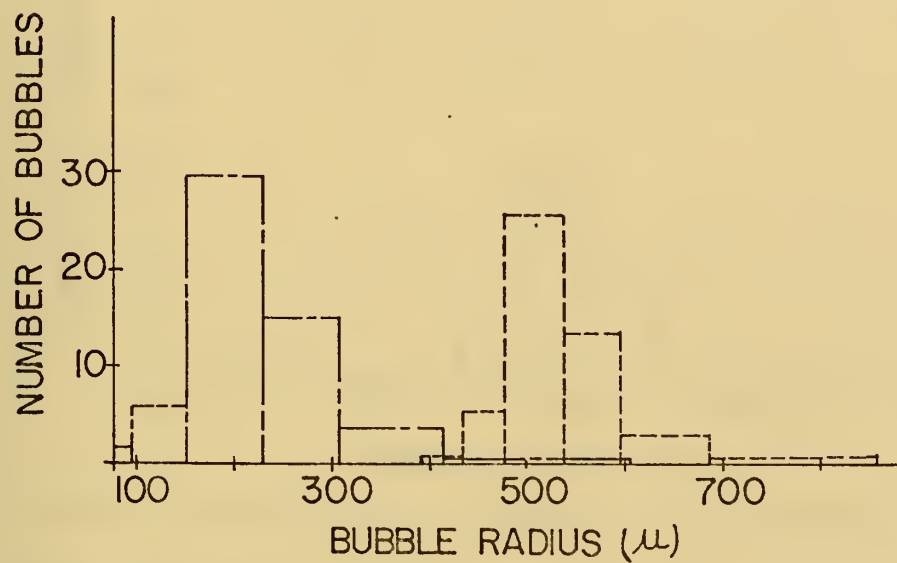
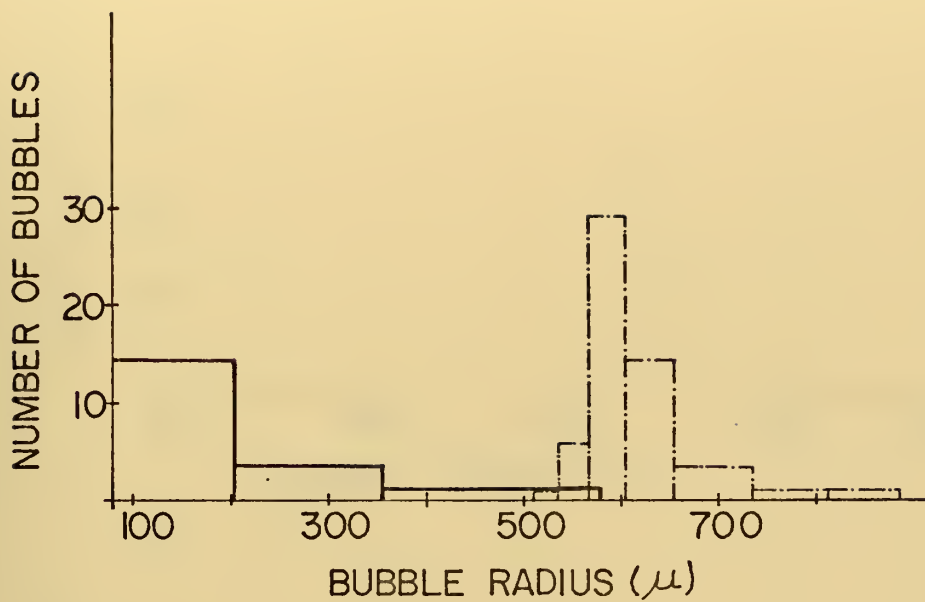




BUBBLE DISTRIBUTION AT HEIGHT = 25 METERS.

Figure 7b



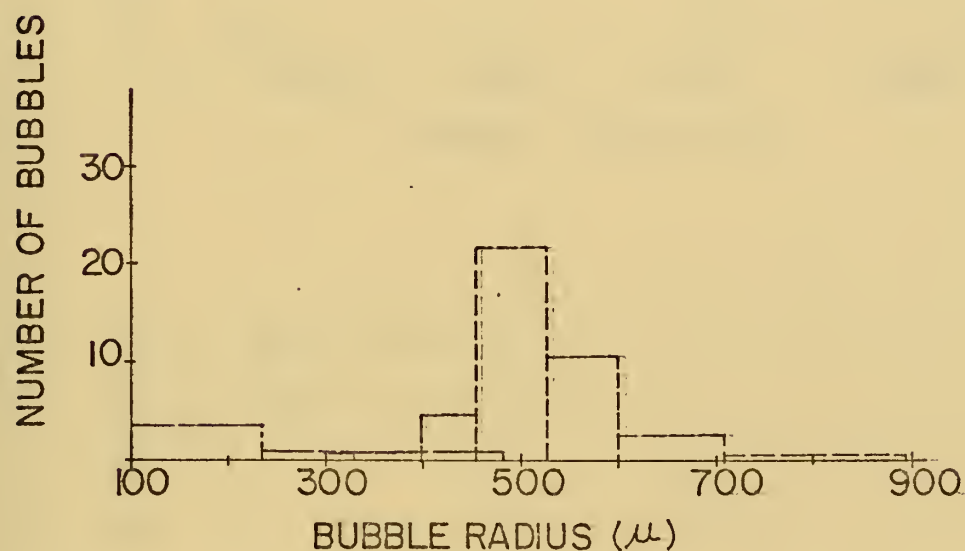
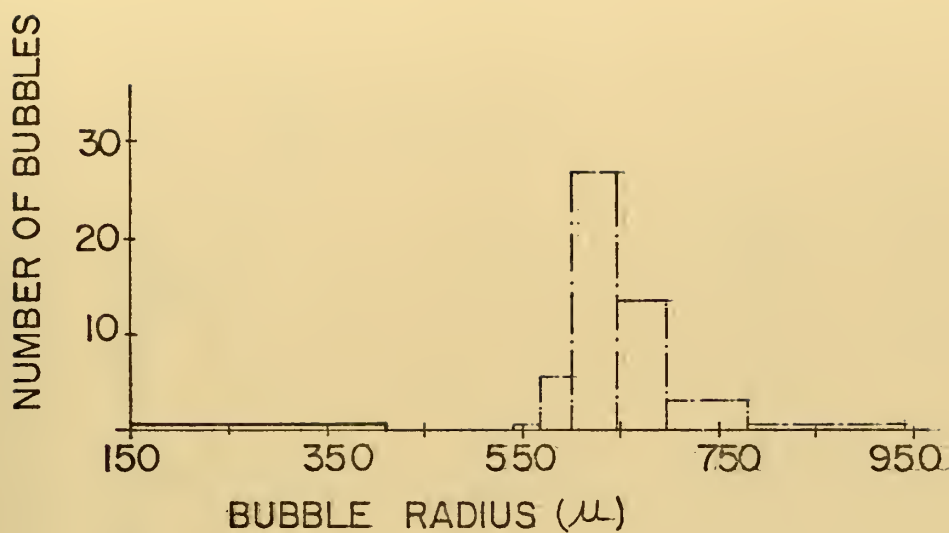


$\overline{H} = \text{solid line}$   
 $\overline{H}_1 = \text{dashed line}$   
 $\overline{H}_2 = \text{dash-dot line}$   
 $\overline{H}_3 = \text{dotted line}$

BUBBLE DISTRIBUTION AT HEIGHT = 50 METERS.

Figure 7c



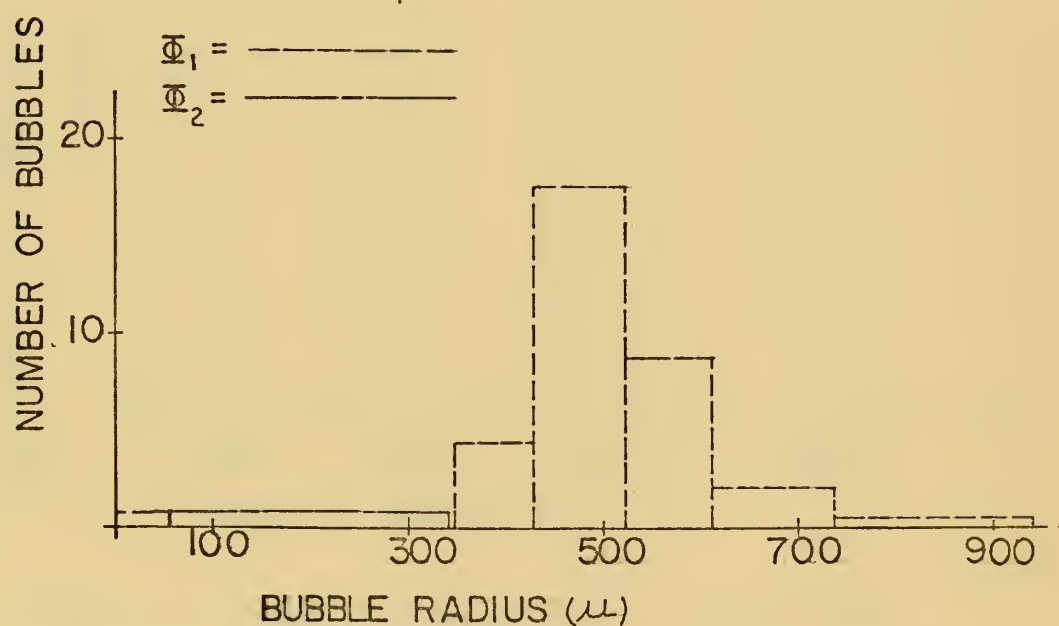
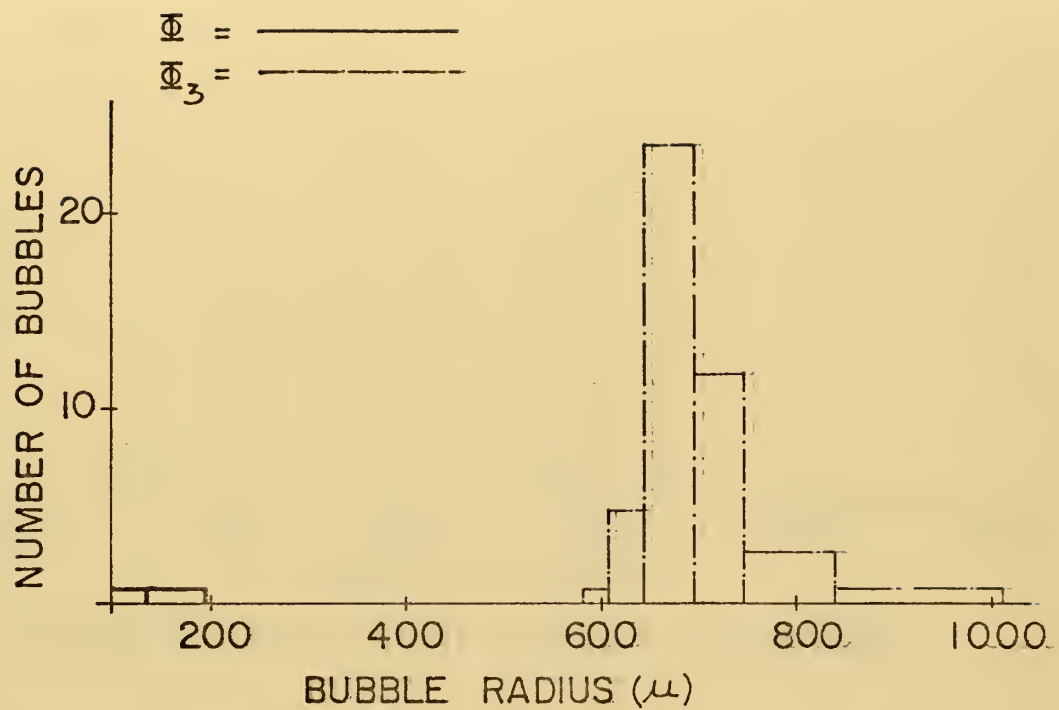


BUBBLE DISTRIBUTION AT HEIGHT = 75 METERS.

$\Phi =$                      
 $\Phi_1 =$                      
 $\Phi_2 =$                      
 $\Phi_3 =$                    

Figure 7d

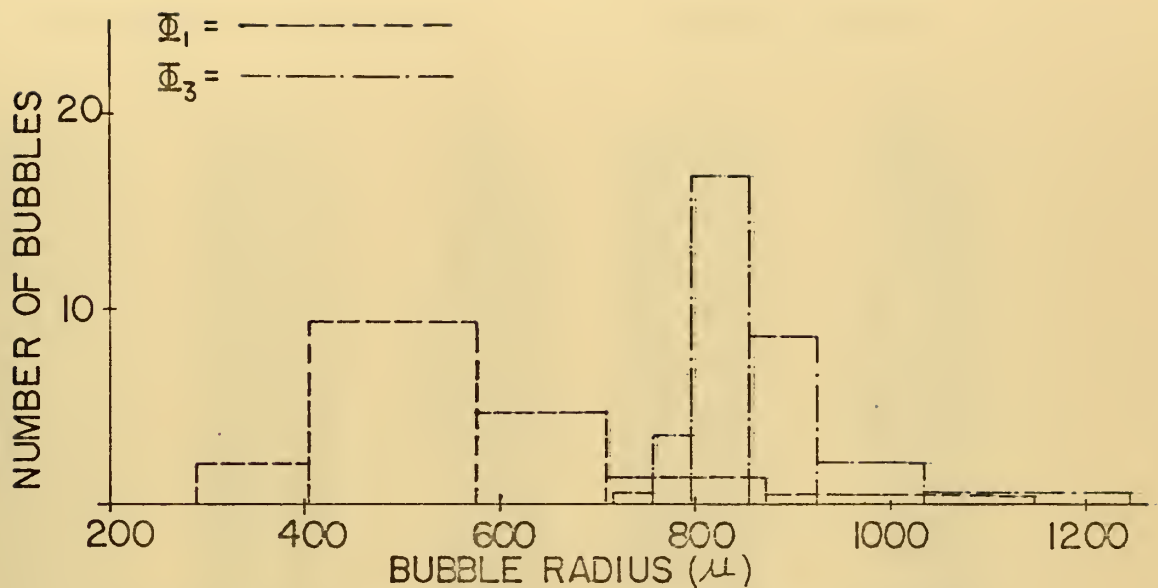




BUBBLE DISTRIBUTION AT HEIGHT = 100 METERS.

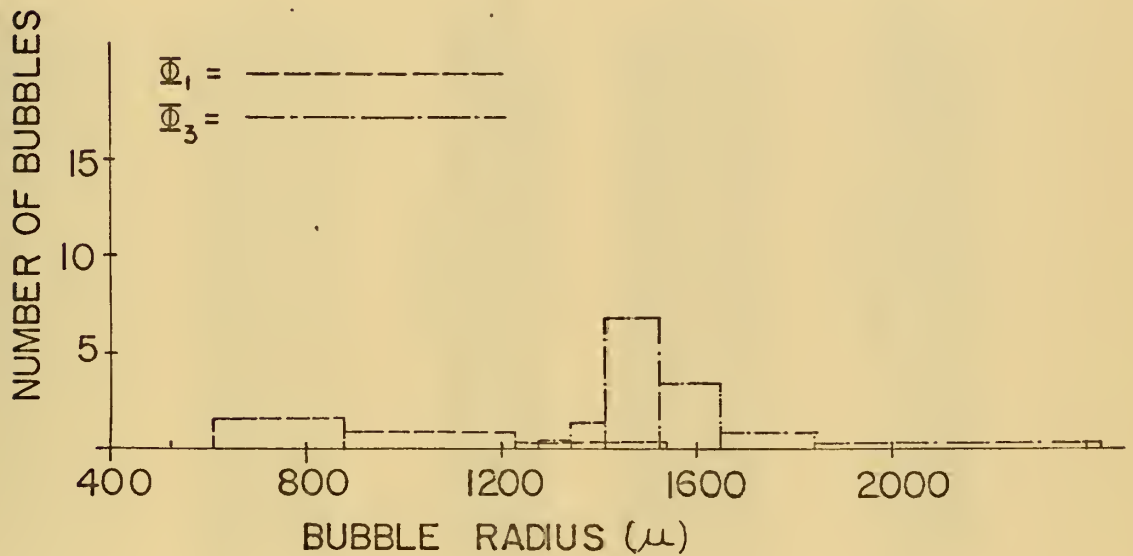
Figure 7e





BUBBLE DISTRIBUTION AT HEIGHT = 150 METERS.

Figure 7f



BUBBLE DISTRIBUTION AT HEIGHT = 197 METERS.

Figure 7g



## COMPUTER OUTPUT

HEIGHT OFF THE BOTTOM = 25.000 METERS

XLO	RADIUS	PHI	RLT3	PHI3
400.000	0.0	0.0	417.535	0.0
465.000	240.062	0.924	485.385	0.929
475.000	258.600	0.925	495.823	0.929
485.000	276.132	0.926	506.261	0.930
490.000	284.593	6.482	511.480	6.509
500.000	301.010	6.486	521.919	6.510
510.000	316.856	6.490	532.357	6.512
515.000	324.596	31.530	537.576	31.633
530.000	347.201	31.552	553.234	31.643
545.000	369.032	31.572	568.892	31.653
555.000	383.230	15.792	579.330	15.830
575.000	410.924	15.802	600.207	15.835
595.000	437.842	15.812	621.083	15.840
600.000	444.469	3.721	626.303	3.727
635.000	489.908	3.724	662.837	3.729
660.000	521.523	3.726	688.933	3.730
670.000	534.007	0.932	699.371	0.933
705.000	577.089	0.932	735.906	0.933
730.000	607.364	0.933	762.002	0.933
740.000	619.375	0.933	772.440	0.933
775.000	661.022	0.933	808.974	0.934
800.000	690.444	0.933	835.070	0.934
810.000	702.146	0.0	845.509	0.0

XLO	RLT1	PHI1	RLT2	PHI2
400.000	338.683	0.0	206.200	0.0
465.000	431.628	0.879	297.174	0.938
475.000	444.714	0.879	310.439	0.938
485.000	457.588	0.879	323.562	0.938
490.000	463.954	6.155	330.075	6.564
500.000	476.556	6.155	343.009	6.564
510.000	489.000	6.155	355.830	6.564
515.000	495.169	29.894	362.201	31.881
530.000	513.480	29.894	391.168	31.881
545.000	531.533	29.894	399.935	31.881
555.000	543.442	14.947	412.346	15.940
575.000	566.997	14.947	436.950	15.940
595.000	590.247	14.947	461.293	15.940
600.000	596.018	3.517	467.342	3.751
635.000	636.015	3.517	509.318	3.751
660.000	664.219	3.517	538.952	3.751
670.000	675.430	0.879	550.735	0.938
705.000	714.391	0.879	591.686	0.938
730.000	741.996	0.879	620.693	0.938
740.000	752.992	0.879	632.244	0.938
775.000	791.303	0.879	672.467	0.938
800.000	818.520	0.879	701.018	0.938
810.000	829.376	0.0	712.401	0.0



HEIGHT OFF THE BOTTOM =

50.000 METERS

XLO	RADIUS	PHI	RLT3	PHI3
400.000	0.0	0.0	438.615	0.0
465.000	0.0	0.0	509.890	0.855
475.000	0.0	0.0	520.855	0.855
485.000	0.0	0.0	531.821	0.856
490.000	0.0	0.0	537.303	0.991
500.000	0.0	0.0	548.269	0.994
510.000	0.0	0.0	559.234	0.997
515.000	0.0	0.0	564.717	29.136
530.000	0.0	0.0	581.165	29.155
545.000	0.0	0.0	597.613	29.174
555.000	0.0	0.0	608.578	14.593
575.000	92.385	14.316	630.509	14.603
595.000	188.945	14.403	652.440	14.613
600.000	204.448	3.393	657.923	3.439
635.000	290.264	3.410	696.301	3.443
660.000	340.102	3.419	723.715	3.445
670.000	358.626	0.855	734.680	0.861
705.000	419.267	0.857	773.059	0.862
730.000	459.715	0.858	800.473	0.863
740.000	475.396	0.859	811.438	0.863
775.000	528.524	0.860	849.817	0.863
800.000	565.120	0.861	877.230	0.864
810.000	579.499	0.0	888.196	0.0

XLO	RLT1	PHI1	RLT2	PHI2
400.000	222.533	0.0	0.0	0.0
465.000	389.746	0.758	0.0	0.0
475.000	408.047	0.758	48.238	0.871
485.000	425.532	0.758	79.764	0.871
490.000	434.014	5.309	93.391	6.096
500.000	450.529	5.309	118.240	6.096
510.000	466.521	5.309	140.916	6.096
515.000	474.345	25.787	151.662	29.610
530.000	497.222	25.787	182.147	29.610
545.000	519.336	25.787	210.647	29.610
555.000	533.722	12.894	228.815	14.805
575.000	561.775	12.894	263.610	14.805
595.000	589.029	12.894	296.797	14.805
600.000	595.736	3.034	304.888	3.484
635.000	641.693	3.034	359.687	3.484
660.000	673.641	3.034	397.238	3.484
670.000	686.252	0.758	411.959	0.871
705.000	729.760	0.758	462.363	0.871
730.000	760.329	0.758	497.464	0.871
740.000	772.455	0.758	511.326	0.871
775.000	814.509	0.758	559.139	0.871
800.000	844.226	0.758	592.707	0.871
810.000	856.048	0.0	606.015	0.0



HEIGHT OFF THE BOTTOM =

75.000 METERS

XLO	RADIUS	PHI	RLT3	PHI3
400.000	0.0	0.0	464.721	0.0
465.000	0.0	0.0	540.238	0.775
475.000	0.0	0.0	551.856	0.776
485.000	0.0	0.0	563.474	0.777
490.000	0.0	0.0	569.283	5.440
500.000	0.0	0.0	580.901	5.444
510.000	0.0	0.0	592.519	5.449
515.000	0.0	0.0	598.328	26.474
530.000	0.0	0.0	615.755	26.502
545.000	0.0	0.0	633.182	26.528
555.000	0.0	0.0	644.800	13.272
575.000	0.0	0.0	668.036	13.288
595.000	0.0	0.0	691.272	13.302
600.000	0.0	0.0	697.081	3.131
635.000	0.0	0.0	737.744	3.136
660.000	0.0	0.0	766.789	3.139
670.000	0.0	0.0	778.407	0.785
705.000	148.353	0.766	819.070	0.786
730.000	244.821	0.772	848.115	0.787
740.000	273.440	0.774	859.734	0.787
775.000	358.003	0.778	900.397	0.788
800.000	410.244	0.780	929.442	0.788
810.000	429.964	0.0	941.060	0.0

XLO	RLT1	PHI1	RLT2	PHI2
400.000	0.0	0.0	0.0	0.0
465.000	331.106	0.638	0.0	0.0
475.000	360.093	0.638	0.0	0.0
485.000	386.043	0.638	0.0	0.0
490.000	398.163	4.464	0.0	0.0
500.000	421.059	4.464	0.0	0.0
510.000	442.507	4.464	0.0	0.0
515.000	452.784	21.681	0.0	0.0
530.000	482.162	21.681	0.0	0.0
545.000	509.784	21.681	0.0	0.0
555.000	527.421	10.841	0.0	0.0
575.000	561.206	10.841	0.0	0.0
595.000	593.406	10.841	12.645	13.575
600.000	601.252	2.551	42.242	3.194
635.000	654.335	2.551	153.845	3.194
660.000	690.674	2.551	212.749	3.194
670.000	704.917	0.638	234.349	0.799
705.000	753.684	0.638	304.416	0.799
730.000	787.663	0.638	350.758	0.799
740.000	801.088	0.638	368.659	0.799
775.000	847.439	0.638	429.073	0.799
800.000	880.028	0.638	470.501	0.799
810.000	892.959	0.0	486.742	0.0



HEIGHT OFF THE BOTTOM =

100.000 METERS

XLO	RADIUS	PHI	RLT3	PHI3
400.000	0.0	0.0	498.412	0.0
465.000	0.0	0.0	579.404	0.690
475.000	0.0	0.0	591.865	0.691
485.000	0.0	0.0	604.325	0.692
490.000	0.0	0.0	610.555	4.846
500.000	0.0	0.0	623.016	4.851
510.000	0.0	0.0	635.476	4.856
515.000	0.0	0.0	641.706	23.599
530.000	0.0	0.0	660.396	23.634
545.000	0.0	0.0	679.087	23.666
555.000	0.0	0.0	691.547	11.843
575.000	0.0	0.0	716.468	11.862
595.000	0.0	0.0	741.388	11.880
600.000	0.0	0.0	747.619	2.796
635.000	0.0	0.0	791.230	2.803
660.000	0.0	0.0	822.380	2.807
670.000	0.0	0.0	834.841	0.702
705.000	0.0	0.0	878.452	0.703
730.000	0.0	0.0	909.603	0.704
740.000	0.0	0.0	922.063	0.704
775.000	0.0	0.0	965.674	0.705
800.000	136.578	0.680	996.825	0.706
810.000	194.535	0.0	1009.285	0.0

XLO	RLT1	PHI1	RLT2	PHI2
400.000	0.0	0.0	0.0	0.0
465.000	219.089	0.517	0.0	0.0
475.000	285.770	0.517	0.0	0.0
485.000	332.348	0.517	0.0	0.0
490.000	351.978	3.618	0.0	0.0
500.000	386.703	3.618	0.0	0.0
510.000	417.224	3.618	0.0	0.0
515.000	431.336	17.575	0.0	0.0
530.000	470.296	17.575	0.0	0.0
545.000	505.502	17.575	0.0	0.0
555.000	527.438	8.787	0.0	0.0
575.000	568.553	8.787	0.0	0.0
595.000	606.878	8.787	0.0	0.0
600.000	616.113	2.068	0.0	0.0
635.000	677.771	2.068	0.0	0.0
660.000	719.318	2.068	0.0	0.0
670.000	735.487	0.517	0.0	0.0
705.000	790.452	0.517	54.319	0.719
730.000	828.450	0.517	147.833	0.719
740.000	843.406	0.517	177.412	0.719
775.000	894.835	0.517	267.406	0.719
800.000	930.829	0.517	324.165	0.719
810.000	945.079	0.0	345.729	0.0



HEIGHT OFF THE BOTTOM =

125.000 METERS

XL0	RADIUS	PHI	RLT3	PHI3
400.000	0.0	0.0	544.643	0.0
465.000	0.0	0.0	633.148	0.596
475.000	0.0	0.0	646.764	0.597
485.000	0.0	0.0	660.380	0.598
490.000	0.0	0.0	667.188	4.191
500.000	0.0	0.0	680.804	4.197
510.000	0.0	0.0	694.420	4.203
515.000	0.0	0.0	701.228	20.428
530.000	0.0	0.0	721.652	20.467
545.000	0.0	0.0	742.076	20.504
555.000	0.0	0.0	755.693	10.264
575.000	0.0	0.0	782.925	10.286
595.000	0.0	0.0	810.157	10.306
600.000	0.0	0.0	816.965	2.426
635.000	0.0	0.0	864.621	2.433
660.000	0.0	0.0	898.661	2.438
670.000	0.0	0.0	912.278	0.610
705.000	0.0	0.0	959.934	0.611
730.000	0.0	0.0	993.974	0.612
740.000	0.0	0.0	1007.590	0.613
775.000	0.0	0.0	1055.246	0.614
800.000	0.0	0.0	1089.287	0.614
810.000	0.0	0.0	1102.903	0.0

XL0	RLT1	PHI1	RLT2	PHI2
400.000	0.0	0.0	0.0	0.0
465.000	0.0	0.0	0.0	0.0
475.000	0.0	0.0	0.0	0.0
485.000	237.512	0.396	0.0	0.0
490.000	281.882	2.773	0.0	0.0
500.000	344.694	2.773	0.0	0.0
510.000	392.070	2.773	0.0	0.0
515.000	412.549	13.469	0.0	0.0
530.000	466.053	13.469	0.0	0.0
545.000	511.787	13.469	0.0	0.0
555.000	539.423	6.734	0.0	0.0
575.000	589.940	6.734	0.0	0.0
595.000	635.914	6.734	0.0	0.0
600.000	646.868	1.585	0.0	0.0
635.000	719.049	1.585	0.0	0.0
660.000	766.966	1.585	0.0	0.0
670.000	785.493	0.396	0.0	0.0
705.000	848.073	0.396	0.0	0.0
730.000	891.037	0.396	0.0	0.0
740.000	907.893	0.396	0.0	0.0
775.000	965.657	0.396	0.0	0.0
800.000	1005.929	0.396	114.088	0.629
810.000	1021.843	0.0	153.122	0.0



HEIGHT OFF THE BOTTOM =

150.000 METERS

XLO	RADIUS	PHI	RLT3	PHI3
400.000	0.0	0.0	614.835	0.0
465.000	0.0	0.0	714.746	0.490
475.000	0.0	0.0	730.116	0.491
485.000	0.0	0.0	745.487	0.492
490.000	0.0	0.0	753.173	3.445
500.000	0.0	0.0	768.544	3.451
510.000	0.0	0.0	783.914	3.458
515.000	0.0	0.0	791.600	16.809
530.000	0.0	0.0	814.656	16.851
545.000	0.0	0.0	837.713	16.890
555.000	0.0	0.0	853.083	8.457
575.000	0.0	0.0	883.825	8.481
595.000	0.0	0.0	914.567	8.502
600.000	0.0	0.0	922.252	2.002
635.000	0.0	0.0	976.050	2.009
660.000	0.0	0.0	1014.478	2.014
670.000	0.0	0.0	1029.848	0.504
705.000	0.0	0.0	1083.646	0.506
730.000	0.0	0.0	1122.074	0.506
740.000	0.0	0.0	1137.445	0.507
775.000	0.0	0.0	1191.243	0.508
800.000	0.0	0.0	1229.670	0.509
810.000	0.0	0.0	1245.041	0.0

XLO	RLT1	PHI1	RLT2	PHI2
400.000	0.0	0.0	0.0	0.0
465.000	0.0	0.0	0.0	0.0
475.000	0.0	0.0	0.0	0.0
485.000	0.0	0.0	0.0	0.0
490.000	0.0	0.0	0.0	0.0
500.000	288.314	1.928	0.0	0.0
510.000	372.655	1.928	0.0	0.0
515.000	404.245	9.362	0.0	0.0
530.000	480.123	9.362	0.0	0.0
545.000	540.491	9.362	0.0	0.0
555.000	575.747	4.681	0.0	0.0
575.000	638.591	4.681	0.0	0.0
595.000	694.510	4.681	0.0	0.0
600.000	707.697	1.101	0.0	0.0
635.000	793.635	1.101	0.0	0.0
660.000	849.981	1.101	0.0	0.0
670.000	871.653	0.275	0.0	0.0
705.000	944.486	0.275	0.0	0.0
730.000	994.222	0.275	0.0	0.0
740.000	1013.686	0.275	0.0	0.0
775.000	1080.214	0.275	0.0	0.0
800.000	1126.462	0.275	0.0	0.0
810.000	1144.711	0.0	0.0	0.0



HEIGHT OFF THE BOTTOM =

175.000 METERS

XLO	RADIUS	PHI	RLT3	PHI3
400.000	0.0	0.0	745.304	0.0
465.000	0.0	0.0	866.416	0.360
475.000	0.0	0.0	885.048	0.361
485.000	0.0	0.0	903.681	0.362
490.000	0.0	0.0	912.997	2.536
500.000	0.0	0.0	931.630	2.542
510.000	0.0	0.0	950.263	2.548
515.000	0.0	0.0	959.579	12.388
530.000	0.0	0.0	987.528	12.427
545.000	0.0	0.0	1015.477	12.464
555.000	0.0	0.0	1034.109	6.244
575.000	0.0	0.0	1071.374	6.266
595.000	0.0	0.0	1108.640	6.286
600.000	0.0	0.0	1117.956	1.480
635.000	0.0	0.0	1183.170	1.487
660.000	0.0	0.0	1229.752	1.492
670.000	0.0	0.0	1248.384	0.373
705.000	0.0	0.0	1313.598	0.375
730.000	0.0	0.0	1360.180	0.376
740.000	0.0	0.0	1378.812	0.376
775.000	0.0	0.0	1444.026	0.377
800.000	0.0	0.0	1490.608	0.378
810.000	0.0	0.0	1509.241	0.0

XLO	RLT1	PHI1	RLT2	PHI2
400.000	0.0	0.0	0.0	0.0
465.000	0.0	0.0	0.0	0.0
475.000	0.0	0.0	0.0	0.0
485.000	0.0	0.0	0.0	0.0
490.000	0.0	0.0	0.0	0.0
500.000	187.500	1.082	0.0	0.0
510.000	382.778	1.082	0.0	0.0
515.000	433.688	5.256	0.0	0.0
530.000	544.064	5.256	0.0	0.0
545.000	625.860	5.256	0.0	0.0
555.000	672.289	2.628	0.0	0.0
575.000	753.476	2.628	0.0	0.0
595.000	824.555	2.628	0.0	0.0
600.000	841.200	0.618	0.0	0.0
635.000	948.866	0.618	0.0	0.0
660.000	1018.887	0.618	0.0	0.0
670.000	1045.730	0.155	0.0	0.0
705.000	1135.654	0.155	0.0	0.0
730.000	1196.856	0.155	0.0	0.0
740.000	1220.771	0.155	0.0	0.0
775.000	1302.382	0.155	0.0	0.0
800.000	1359.016	0.155	0.0	0.0
810.000	1381.344	0.0	0.0	0.0



HEIGHT OFF THE BOTTOM =

197.000 METERS

XLO	RADIUS	PHI	RLT3	PHI3
400.000	0.0	0.0	1098.289	0.0
465.000	0.0	0.0	1276.761	0.196
475.000	0.0	0.0	1304.219	0.197
485.000	0.0	0.0	1331.676	0.197
490.000	0.0	0.0	1345.404	1.384
500.000	0.0	0.0	1372.862	1.389
510.000	0.0	0.0	1400.319	1.393
515.000	0.0	0.0	1414.048	6.775
530.000	0.0	0.0	1455.233	6.803
545.000	0.0	0.0	1496.419	6.829
555.000	0.0	0.0	1523.876	3.423
575.000	0.0	0.0	1578.791	3.438
595.000	0.0	0.0	1633.705	3.453
600.000	0.0	0.0	1647.434	0.813
635.000	0.0	0.0	1743.534	0.818
660.000	0.0	0.0	1812.177	0.822
670.000	0.0	0.0	1839.635	0.206
705.000	0.0	0.0	1935.735	0.207
730.000	0.0	0.0	2004.378	0.207
740.000	0.0	0.0	2031.835	0.208
775.000	0.0	0.0	2127.936	0.208
800.000	0.0	0.0	2196.579	0.209
810.000	0.0	0.0	2224.036	0.0

XLO	RLT1	PHI1	RLT2	PHI2
400.000	0.0	0.0	0.0	0.0
465.000	0.0	0.0	0.0	0.0
475.000	0.0	0.0	0.0	0.0
485.000	0.0	0.0	0.0	0.0
490.000	0.0	0.0	0.0	0.0
500.000	0.0	0.0	0.0	0.0
510.000	527.833	0.338	0.0	0.0
515.000	611.460	1.643	0.0	0.0
530.000	784.567	1.643	0.0	0.0
545.000	909.296	1.643	0.0	0.0
555.000	979.561	0.821	0.0	0.0
575.000	1101.499	0.821	0.0	0.0
595.000	1207.712	0.821	0.0	0.0
600.000	1232.532	0.193	0.0	0.0
635.000	1392.713	0.193	0.0	0.0
660.000	1496.637	0.193	0.0	0.0
670.000	1536.438	0.048	0.0	0.0
705.000	1669.648	0.048	0.0	0.0
730.000	1760.222	0.048	0.0	0.0
740.000	1795.598	0.048	0.0	0.0
775.000	1916.269	0.048	0.0	0.0
800.000	1999.965	0.048	0.0	0.0
810.000	2032.955	0.0	0.0	0.0



## COMPUTER PROGRAM

```

IMPLICIT REAL*8 (A-H,O-Z)
DIMENSION Y(2,5),THTA(4),A(4,4),XL0(25),ZPRT(20),
ISZ(25,10),SXLO(25),SY2(25,10),SPHI(25,10),
2SRLTI(25,10),SPHI1(25,10),SPLT2(25,10),SPHI2(25,10),
4SRLT3(25,10),SPHI3(25,10),FY(2,5),AZDEL(1)
F1(ZZ,Y1,Y2,DVT)=((((2*GAM/(Y2*Y2))*(Y2-(3*RTDEL/Y1)
1*(GAM/Y2-ZZ))/(3*(D-ZZ)+2*GAM/Y2))+(1+(3*RTDEL/Y1)
2*(GAM/(Y2*Y2)+(GAM/Y2-ZZ)*DVT/Y1)))/(3*(D-ZZ)+
32*GAM/Y2)
F2(ZZ,Y1,Y2)=(Y2*Y2-(3*RTDEL*(GAM-(ZZ*Y2))/Y1))/(3*Y2
1*(D-ZZ)+2*GAM)
C THIS PROGRAM USES THE OPTIMAL RUNGE-KUTTA INTEGRATION
C METHOD.
101 READ(5,101) GRAV,BETA,ALPH,D,RTDEL,GAM,XAC
  FORMAT(8E10.3)
READ(5,101) ZMAX,Z0
C Z0 IS THE DEPTH AT WHICH THE SOURCE IS LOCATED..
C ZMAX IS THE SURFACE DEPTH--HERE IT IS ZERO..
READ(5,101) (THTA(J),J=1,4)
READ(5,101) ((A(I,J),J=1,4),I=1,4)
C THE 'A' AND 'THTA' ARRAYS ARE USED FOR THE RUNGE-KUTTA INTEGRATION.
WRITE(6,666)
666 FORMAT('1')
WRITE(6,630) GRAV,BETA,ALPH,D,RTDEL,GAM,XAC
630 FORMAT('0',7(5X,E10.3))
WRITE(6,633) ZMAX,Z0
633 FORMAT(15X,'ZMAX = ',E10.3,'Z0 = ',E10.3)
WRITE(6,634) (THTA(J),J=1,4)
634 FORMAT(4(5X,E10.3))
WRITE(6,635) ((A(I,J),J=1,4),I=1,4)
635 FORMAT(4E15.3)
READ(5,130) NZDEL,NSKP,NXLO,NZPRT
C NZDEL IS THE NUMBER OF INCREMENTS FOR INTEGRATION..
C NSKP IS A DEBUGGING VARIABLE USED TO LIMIT THE
C LINES OF OUTPUT.
C NXLO IS THE NUMBER OF BUBBLES OF DIFFERENT INITIAL
C RADII TO BE ANALYZED.
C NZPRT IS THE NUMBER OF DEPTHS FOR WHICH COMPARISON
C DATA IS TO BE OUTPUTTED.
130 FORMAT(8I10)
READ(5,101) (AZDEL(J),J=1,NZDEL)
C AZDEL IS THE INCREMENT FOR INTEGRATION..
WRITE(6,800) NZDEL,NSKP,NXLO,NZPRT
800 FORMAT(15X,'NZDEL = ',I8,'NSKP = ',I8,'NXLO = ',I8,'NZPRT = ',I8)
WRITE(6,802) (AZDEL(J),J=1,NZDEL)
802 FORMAT('THE AZDEL ARE ',/,8E15.3)
READ(5,101) (XL0(J),J=1,NXLO)
C XL0 IS THE INITIAL BUBBLE RADIUS.
WRITE(6,631) (XL0(J),J=1,NXLO)
631 FORMAT('0','THE INITIAL RADIUS ARE',/,5X,10E12.3)
READ(5,101) (ZPRT(J),J=1,NZPRT)
C ZPRT IS THE DEPTH FOR WHICH COMPARISON DATA IS TO BE
C OUTPUTTED.
WRITE(6,632) (ZPRT(J),J=1,NZPRT)
632 FORMAT('0','THE INPUT HEIGHTS ARE',/,5X,10E12.3)
GB=GRAV/BETA
C NOW COMPUTE THE INITIAL BUBBLE VELOCITY.
DC 80 K=1,NXLO
DD2=DSQRT(XL0(K))
DD3=RTDEL/DSQRT(GB/XAC)
CALL PHIS(XL0(K),PHIC)
VT10=GB*XL0(K)*XL0(K)/ALPH
VT20=DSQRT(GB*XL0(K)/XAC)
VT0=((-1.0+(1.0+(4.0*VT10*VT10)/(VT20*VT20))
1**0.500000)/
2*((2.0*VT10*VT10)/(VT20*VT20)))*VT10.
VO=VT0
C GB IS GRAV DIVIDED BY BETA.
SXLO(K)=XL0(K)*107
C ALL VARIABLES BEGINNING WITH S ARE STORAGE ARRAYS

```



```

C FOR THE FINAL OUTPUT.
C NOTE THAT RADII ARE READ IN AS METERS BUT OUTPUTTED
C IN MICRONS.
C Y(1,1)=0.
C Y(2,1)=XL0(K)
C IFLG=0
C DO 45 I=1,2
C DO 46 J=1,4
C FY(I,J)=0.
C 46 CONTINUE
C 45 CONTINUE
C WRITE(6,636) GB,VT0,VO,VT10,VT20
C 636 FORMAT('1',2X,'GB = ',E12.5,' VT0 = ',E12.5,' VO = ',E12.5,
C 1 E12.5,
C 2 ' VT10 = ',E12.5,' VT20 = ',E12.5)
C WRITE(6,637) (Y(J,1),J=1,2)
C 637 FORMAT(10X,6(3X,E12.5))
C Z=Z0
C KK=1
C KKK=0
C HHT=0.0
C HHT IS THE HEIGHT OFF THE BOTTOM--IT IS EQUAL TO Z-Z0..
C ISO=0
C VT=VT0
C I2=0
C ZTLDY=Z0
C WRITE(6,600) VO,SXLO(K),Z0,ZTLDY,VT0
C 600 FORMAT('0',11X,20X,' VO = ',E10.3,' METERS/SEC ',1,
C 120X,
C 2 ' LO = ',E10.3,' MICRONS ',4,20X,' Z0 = ',F10.3,
C 3 ' METERS ',/,1
C 4 20X,' ZTLDY = ',F10.3,' METERS ',//,20X,' VO TERMINAL = '
C 5 ' ',1
C 6 E10.3,' METERS/SEC')
C WRITE(6,666)
C II=0
C IS=0
C XXLO=XL0(K)*.1D7
C 701 II=II+1
C ZDEL=AZDEL(1)
C IS=IS+1
C IF(IFLG.EQ.1) GO TO 661
C 99 DO 23 J=1,4
C VT1=GB*Y(2,J)*Y(2,J)/ALPH
C VT2=DSQRT(GB*Y(2,J)/XAC)
C VTR2=VT1*VT1/(VT2*VT2)
C VT=(-1.+DSQRT(1.+4.*VTR2))/(2.*VTR2)*VT1
C DVT IS DVT/DL (A DERIVATIVE)
C DVT=(3*VT1/Y(2,J))/(1+4*VTR2)**0.500000-VT/Y(2,J)
C THE INTEGRATION IS DONE HERE.
C FY(1,J)=F1(Z+THTA(J)*ZDEL,VT,Y(2,J),DVT)
C FY(2,J)=F2(Z+THTA(J)*ZDEL,VT,Y(2,J))
C DO 25 N=1,2
C Y(N,J+1)=Y(N,1)+(A(J,1)*FY(N,1)+A(J,2)*FY(N,2)+A(J,3)
C 1*FY(N,3)+1
C 2 A(J,4)*FY(N,4))*ZDEL
C WHEN THE RADIUS Y(2,J) IS LESS THAN ZERO, IFLG IS
C SET TO ONE AND THE INTEGRATING STEPS ARE SKIPPED
C FOR THE REST OF THE PROGRAM.
C IF(Y(N,J+1).LT.0.) GO TO 661
C 25 CONTINUE
C 23 CONTINUE
C Y(1,1)=Y(1,5)
C Y(2,1)=Y(2,5)
C GO TO 662
C 661 Y(1,1)=1.
C Y(2,1)=0.
C IFLG=1
C PHI=0.
C 662 Z=Z+ZDEL
C IF(Z.GT..100D-01) GO TO 999
C HHT=HHT+ZDEL

```



```

IF (IS.EQ.NSKP) GO TO 28
GO TO 701
28 IS=0
IF (IFLG.EQ.1) GO TO 663
VT1=GB*Y(2,1)*Y(2,1)/ALPH
VT2=DSQRT(GB*Y(2,1)/XAC)
VTR2=VT1*(VT2*VT2)
VT=(-1.+DSQRT(1.+4.*VTR2))/(2.*VTR2)*VT1
GAM77=DEXP(Y(1,1))
PHI=VT0*PHI0/(VT*GAM77)
C PHI IS THE GENERAL CASE DISTRIBUTION.
663 RZ=(D-Z)/(D-Z0)
DD11=DSQRT((D-Z0)/(D-Z))
RLT1=(DD11*XLO(K)*XLO(K)*XLO(K)+1.5*ALPH*RTDEL
1*(Z-Z0*Z0)/(GB*(D-Z)))
IF (RLT1.LT..1D-18) RLT1=0.
RLT1=RLT1**0.333333333333
PHI1=PHI0*RZ
C PHI1 IS FOR THE VISCOS DRAG MODEL.
IF (RLT1.EQ.0.0) PHI1=0.0
RLT2=(DD1*DD2*DD2*DD2+DD3*((D-Z)*(1.-DD1*DD1*DD1)-3.
1*D*(1.-DD1)))
IF (RLT2.LT..1D-09) RLT2=0.
RLT2=RLT2**0.666666666666
PHI2=PHI0*DSQRT(RZ)
C PHI2 IS FOR THE TURBULENT DRAG, SURFACE ACTIVE
C MATERIALS MODEL.
IF (RLT2.EQ.0.0) PHI2=0.0
RZ3=RZ**0.333333333333
RLT3=XLO(K)/RZ3
VT13=GB*RLT3*RLT3/ALPH
VT23=DSQRT(GB*RLT3/XAC)
VTR3=VT13*VT13/(VT23*VT23)
VT3=(-1.+DSQRT(1.+4.*VTR3))/(2.*VTR3)*VT13
PHI3=PHI0*VT0*RZ3/VT3
C PHI3 IS FOR THE NO GAS DIFFUSION CASE.
Y2=Y(2,1)*1.D6
XXXX=DABS(HHT-ZPRT(KK))
RRLT1=RLT1*.1D7
RRLT2=RLT2*.1D7
RRLT3=RLT3*.1D7
IF (XXXX.GT.(0.1*ZDEL)) GO TO 223
KKK=KKK+1
SZ(K,KKK)=Z
SY2(K,KKK)=Y(2,1)*.1D7
SPHI(K,KKK)=PHI
SRLT1(K,KKK)=RLT1*.1D7
SPHI1(K,KKK)=PHI1
SRLT2(K,KKK)=RLT2*.1D7
SPHI2(K,KKK)=PHI2
SRLT3(K,KKK)=RLT3*.1D7
SPHI3(K,KKK)=PHI3
KK=KK+1
223 GO TO 701
999 CONTINUE
80 CONTINUE
DO 81 KKK=1,NZPRT
WRITE(6,82)
82 FORMAT('1')
WRITE(6,83) ZPRT(KKK)
83 FORMAT('0',/////,30X,' HEIGHT OFF THE BOTTOM = ',1F13.3,' METERS ',//)
WRITE(6,90)
90 FORMAT(23X,' XLO ',' RADIUS ',' PHI ','1'
1' PLT3 ',' PH13 ')
DO 85 K=1,NXLO
WRITE(6,86) SXLO(K),SY2(K,KKK),SPHI(K,KKK),
1SRLT3(K,KKK),SPHI3(K,KKK)
85 CONTINUE
WRITE(6,92)
92 FORMAT('0',//)

```



```

91 WRITE(6,91)
      FORMAT(23X,'      XLO  ','      RLT1 ','      PHI1 ',
      1'      RLT2','      PHI2')
      DO 87 K=1,NXLO
      WRITE(6,86)  SXLO(K),SRLT1(K,KKK),SPHI1(K,KKK),
      1SRLT2(K,KKK),SPHI2(K,KKK)
86 FORMAT(23X,5F11.3)
87 CONTINUE
81 CONTINUE
      STOP
      END

C
      SUBROUTINE PHIS(R,PHI0)
      IMPLICIT REAL*8 (A-H,O-Z)
      R IS MEASURED IN METERS
      IF(R.LT..4650D-03) GO TO 1
      IF((R.GE..4650D-03).AND.(R.LT..4900D-03)) GO TO 2
      IF((R.GE..4900D-03).AND.(R.LT..5150D-03)) GO TO 3
      IF((R.GE..5150D-03).AND.(R.LT..55500D-03)) GO TO 4
      IF((R.GE..5550D-03).AND.(R.LT..6000D-03)) GO TO 5
      IF((R.GE..6000D-03).AND.(R.LT..6700D-03)) GO TO 6
      IF((R.GE..6700D-03).AND.(R.LT..7400D-03)) GO TO 7
      IF((R.GE..7400D-03).AND.(R.LT..8100D-03)) GO TO 8
      IF(R.GE..8100D-03) GO TO 9
1  PHI0=0.
      GO TO 10
2  PHI0=1.
      GO TO 10
3  PHI0=7.
      GO TO 10
4  PHI0=34.
      GO TO 10
5  PHI0=17.
      GO TO 10
6  PHI0=4.
      GO TO 10
7  PHI0=1.
      GO TO 10
8  PHI0=1.
      GO TO 10
9  PHI0=0.
10 CONTINUE
      RETURN
      END

```



## LIST OF REFERENCES

1. Levich, V. G., Physicochemical Hydrodynamics, Prentice-Hall, 1962.
2. Medwin, H., "Insitu Acoustic Measurements of Bubble Population in Coastal Ocean Waters," Journal of Geophysical Research, v. 75, p. 599-611, January, 1970.
3. Blanchard, D. C. and Woodcock, A. H., "Bubble Formation and Modification in the Sea and Its Meteorological Significance," Tellus, v. 9, p. 143-158, May 1957.
4. McCartney, B. S. and Bary, B. McK., "Echo-Sounding on Probable Gas Bubbles from the Bottom of Saanich Inlet, British Columbia," Deep-Sea Research, v. 12, p. 285-294, 1965.
5. Garrettson, G. A., "Bubble Transport in the Upper Ocean," paper to be submitted to Journal of Fluid Mechanics.
6. Case, K. M. and Zweifel, P. F., Linear Transport Theory, Addison-Wesley, 1967.
7. Wing, G. M., An Introduction to Transport Theory, Wiley, 1962.
8. Wyman, J., Jr., and others, "On the Stability of Gas Bubbles in Sea Water," Journal of Marine Research, v. 11, p. 47-62, July, 1952.
9. LeBlond, P. H., "Gas Diffusion from Ascending Gas Bubbles," Journal of Fluid Mechanics, v. 35, p. 711-719, 1964.
10. Hiestand, F. H., Bubble Distribution in the Upper Ocean, Master's Thesis, Naval Postgraduate School, 1971.
11. Ceschino, F. and Kuntzmann, Jr., Numerical Solutions of Initial Value Problems, Prentice-Hall, 1966.
12. Haderlie, E. C., Professor, Oceanography, conversation with author at Naval Postgraduate School on 18 May 1972.



INITIAL DISTRIBUTION LIST

	No. Copies
1. Defense Documentation Center Cameron Station Alexandria, Virginia 22314	21
2. Library, Code 0212 Naval Postgraduate School Monterey, California 93940	21
3. Asst. Professor G. A. Garrettson, Code 61Gr Department of Physics Naval Postgraduate School Monterey, California 93940	11
4. Professor H. Medwin, Code 61Md Department of Physics Naval Postgraduate School Monterey, California 93940	11
5. LT Thomas C. Vajda, USN 331 W. Ellis Avenue Inglewood, California 90302	11



## DOCUMENT CONTROL DATA - R &amp; D

(Security classification of title, body of abstract and indexing annotation must be entered when the overall report is classified)

## 1. ORIGINATING ACTIVITY (Corporate author)

Naval Postgraduate School  
Monterey, California 93940

## 2a. REPORT SECURITY CLASSIFICATION

Unclassified

## 2b. GROUP

## 3. REPORT TITLE

Bubble Distributions in a Quiescent Ocean Calculated from the Bubble Transport Equation

## 4. DESCRIPTIVE NOTES (Type of report and, inclusive dates)

Master's Thesis, June 1972

## 5. AUTHOR(S) (First name, middle initial, last name)

Thomas C. Vajda

## 6. REPORT DATE

June 1972

## 7a. TOTAL NO. OF PAGES

53

## 7b. NO. OF REFS

12

## 8a. CONTRACT OR GRANT NO.

## b. PROJECT NO.

c.

d.

## 8b. ORIGINATOR'S REPORT NUMBER(S)

## 9b. OTHER REPORT NO(S) (Any other numbers that may be assigned this report)

## 10. DISTRIBUTION STATEMENT

Approved for public release; distribution unlimited.

## 11. SUPPLEMENTARY NOTES

## 12. SPONSORING MILITARY ACTIVITY

Naval Postgraduate School  
Monterey, California 93940

## 13. ABSTRACT

A bubble transport equation was developed and a formal solution obtained for the bubble distribution function. The distribution function obtained depends upon the model used for bubble drag, gas diffusion, and ocean circulation. As a specific application, solutions were obtained for a one-dimensional, quiescent, steady state ocean with a bottom source at 197 meters. The characteristic equations were integrated numerically to test the accuracy of approximate analytical solutions. The calculated bubble densities were compared with experimental data available for this problem. When gas diffusion is neglected, the theoretical and experimental distributions are in general agreement.



14 KEY WORDS	LINK A		LINK B		LINK C	
	ROLE	WT	ROLE	WT	ROLE	WT
Bubbles						
Bubble Distribution						
Transport Equation						
Quiescent Ocean						
Bubble Transport						







6 OCT 80

26560

Thesis

135497

V125 Vajda

c.1 Bubble distributions  
in a quiescent ocean cal-  
culated from the bubble  
transport equation.

6 OCT 80

26560

Thesis

135497

V125 Vajda

c.1 Bubble distributions  
in a quiescent ocean cal-  
culated from the bubble  
transport equation.

thesV125  
Bubble distributions in a quiescent ocea



3 2768 001 88965 2  
DUDLEY KNOX LIBRARY